Published in final edited form as:

Anesthesiology. 2023 December 01; 139(6): 840–857. doi:10.1097/ALN.0000000000004735.

Contribution of μ opioid receptor-expressing dorsal horn interneurons to neuropathic pain-like behavior in mice

Yanmei Qi, PhD[1], **Tyler S. Nelson, PhD**[1], **Pranav Prasoon, PhD**[1], **Christopher Norris, PhD**[1], **Bradley K. Taylor, PhD**[1]

[1]Department of Anesthesiology and Perioperative Medicine, Center for Neuroscience, Pittsburgh Center for Pain Research, Pittsburgh Project to end Opioid Misuse, University of Pittsburgh School of Medicine, Pittsburgh, PA, USA

Abstract

Background: Intersectional genetics have yielded tremendous advances in our understanding of molecularly-identified subpopulations and circuits within the dorsal horn in neuropathic pain. We tested the hypothesis that spinal μ opioid receptor-expressing interneurons (Oprm1-INs) contribute to behavioral hypersensitivity and neuronal sensitization in the spared nerve injury model in mice.

Methods: We coupled the use of Oprm1^{Cre} transgenic reporter mice with whole cell patch clamp electrophysiology in lumbar spinal cord slices to evaluate the neuronal activity of Oprm1-INs in the spared nerve injury (SNI) model of neuropathic pain. We used a chemogenetic approach to activate or inhibit Oprm1-INs, followed by the assessment of behavioral signs of neuropathic pain.

Results: We reveal that SNI yielded a robust neuroplasticity of Oprm1-INs. SNI reduced *Oprm1* gene expression in the dorsal horn as well as the responsiveness of Oprm1-INs to the selective μ agonist DAMGO. SNI sensitized Oprm1-INs, as reflected by an increase in their intrinsic excitability (rheobase: Sham 38.62 ± 25.87 pA (n=29); SNI 18.33 ± 10.29 pA (n=29), p=0.0026) and spontaneous synaptic activity (sEPSC frequency in delayed firing neurons: sham 0.81 ± 0.67 Hz (n=14); SNI 1.74 ± 1.68 Hz (n=10), p=0.0466) and light brush-induced co-expression of the immediate early gene product, Fos in lamina I-II (%Fos/tdT+: sham 0.42 ± 0.57% (n=3); SNI 28.26 ± 1.92% (n=3), p=0.0001). Chemogenetic activation of Oprm1-INs produced mechanical hypersensitivity in uninjured mice (Saline: 2.91 ± 1.08g (n=6); CNO 0.65 ± 0.34 g (n=6), p=0.0006), while chemogenetic inhibition reduced behavioral signs of mechanical hypersensitivity (Saline: 0.38 ± 0.37 g (n=6); CNO 1.05 ± 0.42 g (n=6), p=0.0052) and cold hypersensitivity (saline 6.89 ± 0.88s (n=5) vs CNO 2.31±0.52s (n=5), p=0.0017).

Conclusions: We conclude that nerve injury sensitizes pronociceptive mu opioid receptor-expressing interneurons in mouse dorsal horn. Non-opioid strategies to inhibit these interneurons might yield new treatments for neuropathic pain.

Corresponding author: Bradley K. Taylor, Ph.D., Mailing Address: 200 Lothrop Street, BST W1455, Pittsburgh, PA, 15213, USA, Phone: 1-303-667-7282, bkt@pitt.edu.

Author Contributions: Y.Q., and B.K.T. designed research; Y.Q., T.S.N, P.P., C.N. performed research; Y.Q., T.S.N, and B.K.T. analyzed data; Y.Q., and B.K.T. wrote the manuscript. B.K.T. received funding for the project; B.K.T. supervised the overall project.

Conflicts of Interest: The authors declare no competing interests.

Introduction

The dorsal horn (DH) of the spinal cord receives nociceptive information from sensory neurons. A complex network of excitatory and inhibitory DH interneurons processes this nociceptive input and then transmits it to the brain. A healthy balance of DH excitation and inhibition permits appropriate somatosensation and acute avoidance to painful stimuli to prevent tissue damage.[1] However, in the setting of peripheral nerve injury, an enduring maladaptive increase in excitability (central sensitization) persists in DH neurons and is hypothesized to mediate chronic neuropathic pain.[2,3] Clinical signs include ongoing pain and hypersensitivity to normally non-painful (allodynia) and painful stimuli (hyperalgesia).[4] The mechanisms by which molecularly-identified subpopulations and circuits within the DH contribute to the processing, gating, and transmission of these abnormal and often pathological sensory sensations[5,6] remain an intense area of investigation. For example, glutamatergic interneurons that express protein kinase C gamma[6], somatostatin[7], cholecystokinin,[6] neurokinin-1 receptor,[8] and neuropeptide Y Y1 receptor,[9] have each been implicated in the development and maintenance of neuropathic pain-like behaviors.[5,6,10]

To date, little is known of the contribution to acute or chronic pain of DH neurons that express the G protein–coupled mu-opioid receptor that is encoded by the *Oprm1* gene. This is a major gap in knowledge because *Oprm1* is densely expressed at key sites of spinal nociceptive transmission and pain modulation, including the central terminals of primary afferents and interneurons in the superficial laminae of the dorsal horn (DH) of the spinal cord.[11,12] Indeed, the analgesic actions of opioids at these sites render them the most prescribed pharmacotherapeutic for severe acute pain.[13,14] To test the hypothesis that spinal MOR interneurons (Oprm1-INs) contribute to the modulation of peripheral nerve injury-induced neuropathic pain, we studied the recently developed *Oprm1*$^{Cre:GFP}$ (Oprm1^{Cre}) mouse line with a combination of approaches including *ex vivo* slice electrophysiology, immunohistochemistry, chemogenetics, and behavior.

Materials and Methods

Animals

Wild-type C57BL/6 mice were obtained from Charles River Laboratories (MA, USA). *Oprm1*$^{Cre:GFP}$ mice[15] were kindly provided by Richard Palmiter lab (University of Washington). Ai14 mice (B6.Cg-*Gt(ROSA)26Sor*$^{tm14(CAG-tdTomato)Hze}$/J; stock #007914) were obtained from The Jackson Laboratory (ME, USA). *Oprm1*$^{Cre:GFP}$ and Ai14 mice were maintained in our in-house colony and first-generation crosses were used for histology, *in situ* hybridization and electrophysiological studies. For electrophysiology experiments, we tested both male and female mice at 5–8 weeks of age. For qPCR experiment, we used both male and female mice at 6–10 weeks of age. For behavioral experiments, we tested only male heterozygote *Oprm1*$^{Cre:GFP}$ transgenic mice at 6–12 weeks of age (25 ± 5 g). All mice were group housed and maintained on a 12/12 hour light/dark cycle in a temperature- (20–22°C) and humidity- (45 ± 10%) controlled room, with food and water provided *ad libitum.* All procedures were approved by the University of Pittsburgh Institutional Animal Care and Use Committee in accordance with IASP and ARRIVE guidelines.

Surgeries

Spared nerve injury: Spared nerve injury (SNI) was performed as previously described.[16] Briefly, mice were anesthetized with isoflurane (5% induction and 2% maintenance) and the left hind limb was shaved and sterilized with 70% ethanol. A small incision was made in the skin and the underlying muscle was spread to expose the underlying sciatic nerve branches. The common peroneal and tibial nerves were ligated with 6.0 silk (Ethicon, Somerville, NJ) and then the knot and adjacent nerve (2 mm) were transected, leaving the sural branch intact. The muscle was sutured with 5.0 vicryl (Ethicon, Somerville, NJ) sutures and the skin were closed with 9 mm metal clips, followed by topical triple antibiotic ointment (Neosporin). Wound clips were removed ~10–12 days post-surgery, and behavioral and immunochemical experiments began 14 days after surgery. Sham surgery was performed in an identical manner with nerve exposure but no ligation or transection. For the electrophysiological experiments from injured or sham mice, the surgery was made on 4 weeks old mice, and patch-clamp recordings were conducted 14–18 days after surgery.

Intraspinal AAV Injections: Adult $MOR^{Cre/+}$ mice were anesthetized with inhaled isoflurane (5% induction and 2% maintenance) and the back was shaved and sterilized with 70% ethanol and 2% chlorhexidine gluconate (ChloraPrep One-Step Applicators). A midline incision was carefully made until the underlying vertebrae were clearly visible. A partial laminectomy was performed to remove the L1 vertebrae overlying the L4 segment of the spinal cord. A glass microelectrode was inserted into three separate locations in the exposed left lumbar spinal cord along the rostral caudal axis. At each injection site the glass microelectrode was lowered to a depth of 300 μm below the dura using a stereotaxic frame. We used a Nanoject III Programmable Nanoliter injector (Drummond) to slowly infuse 333.3nL of virus into each of the three spots (3nL/sec) with a 5-minute wait time after completion of each injection to permit adequate infusion. The *lassimus dorsi* was sutured with 5–0 nylon sutures to protect the exposed spinal cord and the overlying skin was closed with 9mm wound clips. Topical triple antibiotic ointment (Neosporin) was applied to the wound. Subcutaneous Buprenorphine HCL (0.05 mg/kg) was utilized for 72 hours as a post-operative analgesic. Behavioral experiments began 21 days after surgery.

Lists of Cre-dependent AAV8 virus used for the chemogenetic experiments: excitatory G-coupled DREADD virus, AAV8-hSyn-DIO-hM3D(G_q)-mCherry (Addgene viral prep # 44361-AAV8; 2.6×10^{13} vg/mL), inhibitory G-coupled DREADD virus, AAV8-hSyn-DIO-hM4D(G_i)-mCherry (Addgene viral prep # 44362-AAV8; 2.3×10^{13} vg/mL) and control virus AAV8-hSyn-DIO-mCherry (Addgene viral prep # 50459-AAV8; 2.2×10^{13} vg/mL).

Behavioral testing

All behavioral measurements were performed by an investigator blinded to experimental treatments by an assistant who randomly assigned treatment groups.

Von Frey test of mechanical sensitivity: Hindpaw 50% mechanical withdrawal thresholds were measured with a calibrated set of 8 von Frey (vF) monofilaments (0.007 to 6 g, Stoelting, Inc, IL, USA). Mice were acclimated to the testing environment within an

acrylic box with opaque walls (15 × 4 × 4 cm) on an elevated wire mesh platform for 45 minutes one day before and immediately prior to behavioral testing. Filaments were applied perpendicular to the lateral hindpaw surface with sufficient force to cause a slight bending of the filament. Testing began with the 0.4 g filament. A positive response was denoted as a rapid withdrawal or licking of the paw within 4 seconds of application. Using an up-down method,[17] a positive response was followed with the next-thinner filament, while a negative response was followed with the next-thicker filament to enable the calculation of 50% withdrawal threshold.

Acetone evaporation test of cold responsiveness: Immediately following von Frey testing, acetone evaporation test was performed on mice in the same acrylic chambers on a raised wire mesh platform. Using a syringe connected to PE-90 tubing, flared at the tip to a diameter of 3 1/2 mm, a drop of acetone was applied to the lateral side of the hind plantar paw. Surface tension maintained the volume of the drop to ~10 μL. The length of time the animal lifted or shook its paw was recorded for 30s. Three observations were averaged.

Hotplate test of heat sensitivity: Mice were placed on a hotplate (Columbus Instruments, USA) at 52.5°C, and the latency to response (jumping, licking, or rapid withdrawal) at either hindpaw was recorded. Withdrawal latency was measured 3 times at 10-min intervals and averaged for each timepoint. A cut-off of 30 s was set to prevent tissue damage

Electrophysiological Recordings

Spinal slice preparation: Acute spinal cord slices were prepared as we have described previously.[18] Briefly, adult mice were anesthetized with 5% isoflurane and perfused transcardially with ice-cold, sucrose-containing artificial cerebrospinal fluid (aCSF) (sucrose-aCSF) that contained (in mM): Sucrose 235, KCl 2.5, KH_2PO_4 1.0, $CaCl_2$ 1, $MgSO_4$ 2.5, $NaHCO_3$ 26, glucose 11, oxygenated with 95% O_2, 5% CO_2. The lumbar spinal cord was rapidly dissected in oxygenated, ice-cold, sucrose-aCSF. After removal of the dura mater, all ventral and dorsal roots, the spinal cord was immersed in low-melting-point agarose (3% in sucrose-aCSF; Life Technologies, Carlsbad, CA, USA). Transverse slices (Lumber segment L3-L5, 300–450 μm) were cut in ice-cold, sucrose-aCSF using a vibrating microtome (7000smz-2; Campden Instruments, Lafayette, IN, USA). All slices were incubated for 15 min at room temperature in recovery solution that contained (in mM): n-methyl-d-glucamine (NMDG) 92, KCl 2.5, NaH_2PO_4 1.2, $NaHCO_3$ 30, HEPES 20, glucose 25, sodium ascorbate 5, thiourea 2, sodium pyruvate 3, $MgSO_4$ 10, $CaCl_2$ 0.5 pH 7.3 (HCl). The slices were then transferred to normal aCSF used for recording, which contained (in mM): NaCl 126, KCl 2.5, NaH_2PO_4 1.25, $CaCl_2$ 2.0, $MgSO_4$ 1.0, $NaHCO_3$ 26, glucose 11, at room temperature for one hour prior to recording.

Patch-clamp recordings: Whole cell patch-clamp recording was performed as we have described previously.[18] Slices were transferred to the recording chamber where it was continuously superfused with oxygenated aCSF. All recordings were made at room temperature on neurons from lamina II, which was visualized as a translucent band across the dorsal horn with differential interference contract (DIC) optics. tdTomato-positive

neurons were detected by epifluorescence. Patch pipettes (3–6 MΩ) were filled with a potassium gluconate based internal solution (in mM): K-gluconate 135, NaCl 1, $MgCl_2$ 2, $CaCl_2$ 1, HEPES 5, EGTA 5, Mg-ATP 2 and Na_4-GTP 0.2, pH 7.3 (~300 mOsm/L). Patch-clamp recordings in current- and voltage-clamp modes were made using an Axon Instruments Multiclamp 700B amplifier (Molecular Devices). The hold potential was −60mV in voltage-clamp mode. Signals were low-pass filtered at 4–20 kHz, amplified 1–20 fold, sampled at 5–10 kHz and analyzed offline using pClamp 11.0.2. Series resistance was less than 30 MΩ. No correction was made for the liquid junction potential (calculated value: −13.9 mV). The resting membrane potential (RMP) was measured immediately after establishing the whole-cell configuration. Neurons that had a resting membrane potential (RMP) positive than −50mV were excluded from the study. The borders of lamina II were set from 20 to 100 μm from the border of the overlying white matter.

Firing patterns during steady-state current injection recordings: As we described previously,[18] firing patterns were determined in response to a series of depolarizing steady-state current injections (1 s duration) with increasing steps of 20 pA. Firing patterns were routinely elicited from resting membrane potential (~−60 mV) and/or hyperpolarized potential (~−80 mV). We elicited firing from hyperpolarized condition to activate the putative partially inactive potassium channels responsible for delayed firing.

Rheobase: The minimum current required to elicit an action potential threshold (rheobase) was measured by means of a current step protocol that was applied to neurons held at RMP, with 5 ms current steps applied in 2.5 pA increments until the appearance of an action potential.

DAMGO-induced currents: DAMGO-induced currents were recorded at −60 mV under voltage-clamp mode. To test the functional responsiveness of Oprm1-expressing neurons, MOR specific agonis DAMGO ([D-Ala^2, N-MePhe^4, Gly-ol]-enkephalin, 1μM) was bath-applied to the soma and inwardly rectifying K^+ currents were evaluated. The peak amplitude of DAMGO-induced current was analyzed from the baseline, $\Delta I > 5$ pA were considered as positive response.

Spontaneous EPSC recordings: Spontaneous excitatory postsynaptic currents (sEPSCs) were recorded at −60 mV in aCSF. For each neuron, sEPSCs were recorded for a total of 3 min. Mini Analysis Program (Synaptosoft) was used to distinguish sEPSC from baseline noise. Initially spontaneous postsynaptic currents were detected automatically by setting appropriate amplitude and area threshold for each recording. Later, all detected events were re-examined and accepted or rejected based on subjective visual examination. Neurons were classified as silent if they failed to display one or more events during the 3-min sampling period and were omitted from the analysis.

qPCR

qPCR was performed as previously described[19]. Briefly, following the decapitation of unanesthetized animals, the spinal cord was extruded by pressure ejection with a blunt 20–22-gauge needle attached to a 10 ml syringe filled with cold saline. The lumbar

enlargement (L3–L5) was removed rapidly. Then, the dorsal horn quadrant ipsilateral to incision was submerged in RNAlater stabilization solution (Thermo Fisher Scientific) and stored at −20°C. First, quadrants were placed in RLT lysis buffer with β-ME, disrupted, and homogenized thoroughly with a rotor-stator homogenizer, and the lysate was centrifuged for 3 min. The supernatant was carefully removed and shifted to a new microcentrifuge tube. One volume of 70% ethanol was added to the lysate, transferred to a RNeasy spin column placed in a 2 ml collection tube, and centrifuged for 15 s at ≥10,000 rpm. Buffer RW1 was added, followed by RPE to wash the spin column membrane, and then centrifuged. Finally, 30 ml RNase-free water was added directly to the spin column membrane and centrifuged for 1 min at ≥10,000 rpm to elute the RNA. The extracted RNA was assessed for yield and purity with a NanoDrop 2000/2000c Spectrophotometer (Thermo Fisher Scientific). All samples were of sufficient yield and purity (260nm/280nm ratio>2.0). To produce a purified cDNA template, extracted RNA samples were reverse transcribed with a SuperScript IV VILO Master Mix with ezDNase Enzyme Kit (catalog #1176050, Invitrogen) using the following thermal cycling steps: (1) anneal primers at 25°C for 10 min, (2) reverse transcribe RNA at 50°C for 10 min, and (3) inactivate enzyme at 85°C for 5 min.

Gene expression of *Orpm1* (Mm01188089_m1, Catalog no: 4331182) and the internal reference gene glyceraldehyde 3-hosphate dehydrogenase GAPDH (Mm99999915_g1) was calculated with Applied Biosystems QuantStudio 3 Real-Time PCR System using TaqMan gene expression probes (Thermo Fisher Scientific). Realtime PCRs included one cycle of predegeneration at 95°C for 30 s, 40 cycles of PCR reaction at 95°C for 5 s, and dissociation at 60°C for 34s. The relative gene expression was calculated based on the 2DD Ct method.[20] The abundance of each transcript was normalized to the internal control housekeeping gene, GAPDH, which rarely changes in response to system perturbation;[21] as expected, spinal cord levels were similar between sham and SNI mice.

In Situ Hybridization, Immunohistochemistry and Microscope imaging

Fluorescence in situ Hybridization: MOR^{Cre} X Ai14 mice were transcardially perfused with 10ml ice-cold 1x PBS and spinal cords were rapidly extracted, embedded in OCT, frozen on dry ice, and stored at −80° C until use. Spinal cords were cryosectioned at 10 μm and mounted directly onto slides (Superfrost Plus, Fisher Scientific). Sections were fixed in chilled 4% PFA for 15 minutes and then dehydrated with increasing ethanol concentrations (50%, 70%, then 100% for 5 min each). Fluorescence *in situ* hybridization was performed using an RNAscope Multiplex Fluorescent Reagent Kit v2 (Advanced Cell Diagnostics, USA; Cat# 323100) following the manufacturer's protocol. Slides were pretreated for 15 minutes with protease (Advanced Cell Diagnostics, USA), and then incubated and hybridized with *Oprm1* mRNA probe (Cat. # 315841) and *tdTomato* mRNA probe (Cat. # 317041) for 2 hours at 40° C in a humidified oven (HybEZ; Advanced Cell Diagnostics, USA). Following a series of signal amplification and rinse steps, slides were washed in 0.01 M phosphate buffer, air-dried and cover-slipped with Hard Set Antifade Mounting Media with DAPI (Vectashield; Vector Labs).

Brush induced Fos expression: To assess Fos expression in sham and SNI animals, a touch stimulation protocol was used 14 days after surgery (Figure 7A). Briefly, mice were

anesthetized with isoflurane (5% induction, 2% maintenance) and the lateral surface of the left hindpaw was gently stroked in the longitudinal plane with a cotton tipped applicator for 3 seconds of every 5 seconds, for 5 minutes. 1 hour after brushing, mice were anesthetized and processed for Fos immunohistochemistry.

Immunohistochemistry: Mice were administered an intraperitoneal injection of sodium pentobarbital (100 mg/kg, 0.2 mL, Fatal-Plus) and perfused with 10% formalin. Spinal cords were collected and postfixed in 10% formalin overnight, then dehydrated in 30% sucrose in 1xPBS for at least two days. L3-L5 lumber segments were sectioned at 20 μm transverse sections using freezing microtome (Leica Biosystems). For Fos immunostaining, sections were blocked in 1xPBS containing 10% normal goat serum (NGS, MP Biomedicals) and 0.3% Triton X-100 (VWR, USA) for 1 hour, and then incubated overnight at −4°C fridge with anti-Fos primary antibody (1:1000; polyclonal Guinea pig anti-cFos; Synaptic Systems, Germany; Cat# 226005) which diluted in 5% NGS and 0.3% Triton X-100. Following three times washing, sections were incubated with AlexaFluor 488-conjugated goat anti guinea pig secondary antibodies (ThermoFisher Scientific) diluted 1:1000 in 1xPBS for 1.5 h at room temperature. For immunostaining with TLX3 and PAX2 antibodies, sections were blocked in 5% normal donkey serum (NGS, MP Biomedicals) and 0.3% Triton X-100 for 1 hour, and then incubated overnight at −4°C fridge with guinea pig anti-TLX3 (1:5,000) kindly given by Carmen Birchmeier and Goat anti-human PAX2 (1:1000; R&D Systems, MN; AF3364) which was diluted in 3% NDS and 0.3% Triton X-100. Sections were then mounted on Superfrost plus slides (ThermoFisher Scientific), washed in 0.1M phosphate buffered deionized water, allowed to dry and then coverslipped with Vectashield + DAPI mounting medium (Vector Laboratories).

Microscopy and Quantification: All images were captured on a Nikon Eclipse Ti2 microscope epifluorescence microscope equipped with a 20x, 0.75 NA and a 40x, 0.95 NA objective and analyzed using NIS-Elements Advanced Research software v5.02 (Nikon, Japan). The same exposure time (60 to 500 ms) was used for all images captured in each channel. Throughout image acquisition and quantification, the investigator, while blind to treatment groups, adjusted brightness and contrast in the same manner for each image. For quantification of FISH, only cells with at least 4 puncta associated with a DAPI nucleus were considered positive; positive cells from five to six spinal cord sections from four mice were counted and averaged. For quantification of immunohistochemistry, ten sections from three mice for each experimental group were counted and averaged.

Experimental Groups:

For the morphine analgesia studies (Figure 1), saline and morphine was administered to wild-type (n=4), heterozygous (n=5), or homozygous (n=4) $Oprm1^{Cre}$ mice. For the MOR expression studies (Figure 2), 4 mice were used. For the electrophysiological recordings of DAMGO-induced outward currents in tdTomato-labelled Oprm1-INs (Figure 3), the two experimental groups were $Oprm1^{tdT}$ positive neurons (17 neurons from 7 mice) and tdTomato-negative neurons (9 neurons from 3 mice). Two or three slices were taken from each mouse, and only one neuron was recorded from each slice. To action potential firing patterns (Figure 4), we recorded 36 neurons from 9 tdTomato-positive mice and 35 neurons

from 6 tdTomato-negative mice. For the *Oprm1* mRNA study with qRT-PCR (Figure 5D–5E), the eight experimental groups were male sham (n=6), male SNI d3 (n=6), male SNI d7 (n=6), male SNI d14 (n=6), female sham (n=6), female SNI d3 (n=6), female SNI d7 (n=6), and female SNI d14 (n=6). For the electrophysiological study of tdTomato-labelled Oprm1-INs (Figures 5–6), the two experimental groups were sham (n=7) and SNI (n=7). For the Fos studies in $Oprm1^{tdT+}$ mice (Figure 7), the two experimental groups were sham (n=3) and SNI (n=3). For the chemogenetic activation study with excitatory G-coupled DREADD virus (Figure 8), the experimental groups were control AAV8-hSyn-DIO-mCherry group (n=8) and AAV8-hSyn-DIO-hM3D(G_q)-mCherry excitatory DREADD group (n=8). For the chemogenetic inhibition study (Figure 9a), all mice received AAV8-hSyn-DIO-hM4D(G_i)-mCherry virus and spared nerve injury, then saline and CNO.

Data Presentation

Graphs and Images were created in GraphPad Prism 9.0., Adobe Illustrator 26.3.1., or Biorender.com.

Statistical analyses

Electrophysiological data were analyzed with Clamp fit 10.3 (Molecular Devices, USA). Statistical analyses were performed in Prism 9.0 (GraphPad Software Inc., USA). Two-tailed Student's t test (unpaired), χ^2 test, Fisher's exact test, one-way analysis of variance (ANOVA) and two-way repeated-measures ANOVA followed by Tukey's and Holm-Sidak post hoc tests were used for statistical comparison. If the Shapiro–Wilk test determined that a set of data was not normally distributed, then the Mann Whitney test was used in place of t test. Group sizes were based on our previous publications with similar experimental designs, rather than power calculation conducted prior to the study. Statistical significance was determined as $*P < 0.05$. The results are expressed as mean ± standard deviation (SD).

Results

Transgenically labelled murine Oprm1-interneurons express functional μ opioid receptors

The $Oprm1^{Cre}$ knock-in/knock-out mouse line was generated by inserting Cre:GFP just 5' of the initiation codon in the first coding exon of the *Oprm1* gene.[15] As illustrated in Figure 1, we evaluated morphine-induced analgesia with a 52.5°C hot plate in wild type (WT), heterozygous ($Oprm1^{Cre/+}$) and homozygous ($Oprm1^{Cre/Cre}$) mice. As expected, morphine significantly increased the withdrawal latency in WT (two-way ANOVA followed by Tukey post hoc test, F (2,20) = 61.50, P<0.0001) but not homozygous mice (two-way ANOVA followed by Tukey post hoc test, F (2,20) = 61.50, P=0.28) mice. Importantly, morphine-induced analgesia was intact in heterozygous mice (two-way ANOVA followed by Tukey post hoc test, F (2,20) = 61.50, P<0.0001), indicating that a single allele is sufficient to maintain MOR function *in vivo*.

To genetically label Oprm1-expressing neurons in the spinal dorsal horn, we crossed the $Oprm1^{Cre}$ mouse line with a *loxp*-flanked tdTomato (Ai14) reporter mouse line, yielding $Oprm1^{tdT}$ mice. As predicted by previous studies,[11] tdTomato-labeled neurons were predominantly distributed throughout laminae I-III of the spinal cord. Next, we determined

whether tdTomato-labeled neurons recapitulate endogenous *Oprm1* expression using double label fluorescence *in situ* hybridization (FISH) with *tdTomato* and *Oprm1* mRNA probes in lumbar spinal cord sections from Oprm1^{tdT} mice. As illustrated in Figure 2, quantitative analysis revealed that the majority (86.7% ± 1.4%) of tdTomato-labelled neurons throughout laminae I-III expressed *Oprm1* mRNA. Similar results were observed when segregating the analysis to laminae I-II (86.2%) and lamina III (87.3%) (Figure 2C). These data indicate that tdTomato reliably labels Oprm1-expressing neurons in the spinal dorsal horn with high fidelity.

We next investigated the functional responsiveness of Oprm1^{tdT} neurons to the μ-selective agonist DAMGO. To this end, we performed whole cell patch-clamp recordings in lumbar spinal cord slices to record from either tdTomato-labelled (Oprm1^{tdT+}) or tdTomato-negative (Oprm1^{tdT-}) neurons (Figure 3A). Consistent with previous literature,[22] bath administration of DAMGO (1 μM, 2 min) produced outward currents in dorsal horn interneurons (Figure 3B). As illustrated in Figure 3C-D, DAMGO induced outward currents in 10 out of 17 Oprm1^{tdT+} neurons, with a mean peak amplitude of 28.94 ± 6.93 pA. As predicted, Oprm1^{tdT-} neurons never responded to DAMGO (9 cells from 3 mice). Similar results were obtained when the data was segregated by sex (Supplemental Figure 1). These data establish that spinal Oprm1^{tdT+} neurons express functional μ opioid receptors.

Neurophysiological and molecular heterogeneity of Oprm1^{tdT} neurons

Superficial dorsal horn INs can be segregated by action potential (AP) firing patterns in response to depolarizing current steps.[23] As illustrated in Figure 4A, we identified four major action potential firing patterns in tdTomato-labelled Oprm1-INs. Consistent with previously published criteria,[18,24,25] neurons were classified as delayed if there was a delay (>100 ms) between the start of the depolarizing step and the first action potential. Transient firing neurons only fired action potentials at the start of the depolarization step. Phasic firing neurons exhibited three or more action potentials immediately after the onset of current injection but terminated before the end of the current pulse. Tonic firing neurons exhibited continuous action potential discharge throughout the depolarizing step.

Figure 4B illustrates the prevalence of the identified firing patterns elicited from RMP (~−60mV) in tdTomato-labelled (Oprm1^{tdT+}) or tdTomato-negative (Oprm1^{tdT-}). From RMP, we found that a smaller percentage of Oprm1^{tdT+} (12/36, ~33%) neurons exhibited delayed firing than Oprm1^{tdT-} (20/35, ~57%) neurons (Fisher's exact testT, p=0.058), and a much higher percentage of Oprm1^{tdT+} (15/36, ~42%) neurons exhibited tonic firing compared to Oprm1^{tdT-} (5/35, ~14%) neurons (Fisher's exact test, p=0.017). The distribution of transient and phasic firing was similar between the two groups. AP discharge patterns are affected by membrane holding potential. For example, detection of a delayed firing pattern often requires current injection from a hyperpolarized holding potential.[18,23] Thus, we analyzed AP firing patterns elicited not only from RMP, but also from a hyperpolarizing potential (~−80mV). When AP firing was evoked from conditioning hyperpolarized potential, the most prevalent AP firing pattern in Oprm1^{tdT+} neurons was delayed firing (15/33, ~45%) followed by tonic (8/33, ~24%), transient (8/33, ~24%) and phasic (2/33, ~6%) (Figure 4C). In contrast, a much higher percentage of Oprm1^{tdT-}

(25/35, ~71%) neurons exhibited delayed firing compared to Oprm1^{tdT+} neurons (Fisher's exact test, p=0.0014). The percentage of tonic firing or transient firing in Oprm1^{tdT-} (4/35, ~11%) neurons was not different with Oprm1^{tdT+} neurons (Fisher's exact test, p=0.21 or p=0.34). Additionally, passive membrane properties, including membrane capacitance, input resistance and resting membrane potential, were similar between Oprm1^{tdT+} and Oprm1^{tdT-} neurons (Table 1). Previous electrophysiological studies in superficial dorsal horn neurons indicated that excitatory interneurons generally exhibit delayed AP firing pattern while inhibitory interneurons most commonly display a tonic AP firing pattern.[26] Thus, our neurophysiological characterization data suggest that Oprm1^{tdT+} neurons contain both excitatory and inhibitory interneurons in the superficial dorsal horn.

In addition to segregation by neurophysiological firing patterns, spinal cord dorsal horn neurons can also be characterized based on their histochemical expression of excitatory or inhibitory neurotransmitters.[10] Originally, immunolabeling with a Oprm1-selective antibody indicated its specific expression in excitatory neurons in the spinal cord dorsal horn.[11] In contrast, recent studies using FISH have revealed that *Oprm1* mRNA is detected in both excitatory and inhibitory interneurons in the dorsal horn.[27–29] To confirm this neurochemical phenotype in our labelled Oprm1^{tdT+} neurons, we conducted double-label immunohistochemistry of tdTomato with the excitatory neuronal marker TLX3 and the inhibitory neuronal marker PAX2. As illustrated in Figure 4D-E, Oprm1^{tdT+} neurons co-expressed both TLX3 and PAX2 (Figure 4D-E). In laminae I-II, Oprm1^{tdT+} colocalization with TLX3 and PAX2 was 59.94 ± 3.31% and 34.96 ± 2.66%, respectively (Figure 4F). Similar expression patterns were found in lamina III (Figure 4F). Thus, Oprm1-INs segregate into excitatory and inhibitory subpopulations.

Nerve injury reduces functional responsiveness of Oprm1-interneuronss to DAMGO

Neuropathic pain arises from a lesion or disease affecting the peripheral or central nervous system. Despite the clear effects of opioids on reducing spinal excitability,[14,22,30,31] peripheral nerve injury reduces DAMGO inhibition of superficial dorsal horn neurons in randomly sampled lamina II neurons.[32] To test this in Oprm1-INs, we recorded DAMGO-induced outward currents in lamina II Oprm1^{tdT+} neurons following SNI. As illustrated in Figure 5A, behavioral testing confirmed that Oprm1^{tdT+}mice developed mechanical hypersensitivity two weeks after SNI surgery (Two tailed unpaired t-test, p<0.0001, n=7). In sham mice, DAMGO (1 μM) induced an outward current in 54.6% (12 out of 22 cells, from 7 mice) of Oprm1^{tdT+} neurons (Figure 5B), however, SNI significantly reduced the proportion of Oprm1^{tdT+} neurons that responded to DAMGO stimulation to 16.7% (Fisher's exact test, p=0.012, 4 out of 24 cells, from 7 mice). The peak amplitude of DAMGO induced currents did not differ between sham and SNI (Figure 5C, Mann Whitney test, p=0.52, n=12 cells from 7 mice in Sham vs n=4 cells from 7 mice in SNI). Similar results were obtained when the data was segregated by sex (Supplemental Figure 2). Consistent with these electrophysiological results, we also observed a robust reduction of *Oprm1* mRNA expression 14 days after SNI in both male (Figure 5D, One-way ANOVA followed by Tukey's post hoc test, F (3, 20) = 13.80, p<0.0001, n=6) and female (Figure 5E, One-way ANOVA followed by Tukey's post hoc test, F (3, 20) = 20.30, p<0.0001, n=6) mice. Overall,

our results suggest that SNI reduces the functional responsiveness of Oprm1-INs to a MOR selective agonist, perhaps via injury-induced downregulation of *Oprm1*.

Nerve injury increases membrane excitability and synaptic activity of Oprm1^{tdT+} neurons

Peripheral nerve injury increases the excitability of spinal dorsal horn neurons by increasing their spontaneous action potential discharge and amplifying neuronal responses to peripheral stimulation.[33,34] However, these studies were restricted to unidentified neurons. To determine whether the Oprm1-IN subpopulation is sensitized after SNI, we investigated intrinsic membrane properties and synaptic activity with whole cell patch clamp recordings of lamina II Oprm1^{tdT+} neurons. As illustrated in Table 2 and Figure 6A, SNI did not change passive membrane properties including membrane capacitance, membrane resistance, input resistance and AP amplitude of Oprm1^{tdT+} neurons. On the other hand, SNI significantly reduced rheobase (Figure 6B, Sham 38.62 ± 25.87 pA (n=29 cells from 7 mice); SNI 18.33 ± 10.29 pA (n=24 cells from 7 mice), Mann Whitney test, p=0.0026) and depolarized the resting membrane potential (Figure 6C, two tailed unpaired t-test, p=0.049, sham: n=30 cells from 7 mice; SNI: n=26 cells from 7 mice), indicating an increased intrinsic excitability.

Previous studies indicate that the ability of peripheral nerve injury to change spontaneous excitatory postsynaptic current (sEPSC), a measure of synaptic activity, is dependent on action potential firing patterns.[24] As illustrated in Fig 6D, the incidence of delayed, transient, phasic and tonic firing patterns was indistinguishable between sham and SNI groups (χ2 test, p=0.25, sham: n=32 cells from 7 mice; SNI: n=26 cells from 7 mice). Based on our previous studies of neuropeptide Y1 receptor-expressing interneurons[9], we segregated delayed firing (DF) from other Oprm1^{tdT+} neurons. Figure 6F shows that SNI did not change sEPSC amplitude in DF (Mann Whitney test, p=0.92, sham: n=14 cells from 7 mice; SNI: n=10 cells from 7 mice) or non-DF neurons (Figure 6F, Mann Whitney test, p=0.60, sham: n=9 cells from 7 mice; SNI: n=7 cells from 7 mice), but increased sEPSC frequency (sham 0.81 ± 0.67 Hz; SNI 1.74 ± 1.68 Hz) in DF neurons (Figure 6G, Mann Whitney test, p=0.046, sham: n=14 cells from 7 mice; SNI: n=10 cells from 7 mice). Similar results were obtained when the data was segregated by sex (Supplemental Figure 3).

Spared nerve injury increased touch-evoked Fos expression in Oprm1^{tdT+} neurons

Expression of the immediate early gene product Fos is a marker of neuronal activity in nociresponsive dorsal horn neurons.[35,36] Peripheral nerve injury alone induces minimal Fos, but primes Fos expression following application of a non-noxious light touch stimulus to the hindpaw.[37] Two weeks after Sham surgery, light brush of the lateral hindpaw with a cotton swab produced minimal Fos expression in laminae I-II (2.86 ± 1.65) or III (2.40 ± 2.01), consistent with previous results indicating minimal baseline Fos in superficial laminae of the mouse.[38] Two weeks after SNI, light brush produced a robust number of Fos^{+} Oprm1^{tdT+} neurons in laminae I-II (45.98 ± 8.05) and lamina III (SNI 35.64 ± 1.82) at side ipsilateral to surgery (Figure 7D, Two-way ANOVA followed by Tukey's post hoc test, F (3, 6) = 90.78, p<0.0001, n=3 mice/group). SNI evoked light brush-evoked Fos in over one-quarter of the Oprm1^{tdT+} neuron population in laminae I-II (%Fos/tdT+: sham 0.42±0.57%; SNI 28.26±1.92%) and lamina III (sham 0.83 ± 0.97%; SNI 26.50 ± 1.52%) (Figure 7E, Two-

way ANOVA followed by Tukey's post hoc test, F (3, 6) = 346.50, p<0.0001, n=3 mice/group).

Chemogenetic activation of spinal Oprm1-interneurons induces mechanical hypersensitivity

Our electrophysiology and Fos studies indicate that SNI increases the excitability and activation of dorsal horn Oprm1-INs. To test the hypothesis that this can generate pain-like behaviors, we injected a Cre-dependent excitatory Designer Receptor Exclusively Activated by Designer Drugs (DREADD, AAV8-hSyn-DIO-hM3D$_{Gq}$-mCherry) into the left lumbar dorsal horn of heterozygous Oprm1^{Cre} mice. Three weeks later, we administered the designer DREADD ligand, clozapine N-oxide (CNO, 3mg/kg, ip) and evaluated nocifensive behaviors (Figure 8). Chemogenetic activation of Oprm1-INs with CNO but not saline reduced mechanical threshold of the ipsilateral (left) hindpaw in mice (Saline: 2.91 ± 1.08g; CNO 0.65 ± 0.34g) that had been injected with the excitatory DREADD (hM3D$_{Gq}$) but not with control (mCherry) virus (Figure 8B, Two-way RM ANOVA followed by Holm Sidak's post hoc test, F (3, 28) = 7.83, p=0.0006, n=8 mice/group). CNO did not change cold response duration (Figure 8C, Two-way RM ANOVA, F (3, 28) = 1.64, p=0.2016, n=8 mice/group) or withdrawal latency to noxious heat (Figure 8D, Two-way RM ANOVA, F (3, 26) = 1.94, p=0.1473, n=8 mice/group). These results demonstrate that chemogenetic activation of spinal Oprm1-INs elicits mechanical but not thermal hypersensitivity in uninjured mice.

Chemogenetic inhibition of spinal Oprm1-interneurons reduces neuropathic pain

Dermorphin-saporin ablation of Oprm1-INs in the rostroventromedial medulla (RVM) inhibited mechanical hypersensitivity after nerve injury, indicating their contribution to neuropathic pain in rats.[39] To test the hypothesis that Oprm1-INs in the DH similarly contribute to neuropathic pain, we intraspinally administered a Cre-dependent inhibitory DREADD (AAV8-hSyn-DIO-hM4D$_{Gi}$-mCherry) into heterozygous Oprm1^{Cre} mice, allowed three weeks for stable viral transfection, and then conducted SNI surgery (Figure 9). As illustrated in Figures 9B-C, mechanical sensitivity and cold response duration increased two weeks later. As illustrated in Figures 9D-E, chemogenetic inhibition of Oprm1-INs with CNO but not saline reduced mechanical (Saline: 0.38 ± 0.37g; CNO 1.05±0.42g, p=0.0052, two-way RM ANOVA followed by Holm Sidak's post hoc test, F (1, 10) = 8.71, p=0.0074, n=6 mice/group) and cold hypersensitivity (saline 6.89 ± 0.88s vs CNO 2.31±0.52s, p=0.0017, two-way RM ANOVA followed by Holm Sidak's post hoc test, F (1, 8) = 3.62, p=0.0017, n=5 mice/group). These data suggest that Oprm1-INs contribute to mechanical and cold allodynia after nerve injury.

Discussion

In the present study we characterized the neurochemical and electrophysiological phenotype of Oprm1-INs in the murine DH and revealed their contribution to the maintenance of neuropathic pain-like behavior. First, we demonstrated that Oprm1-INs express excitatory and inhibitory neuronal markers in the DH and display four distinct firing patterns in response to steady-state depolarizing current injection. Second, the responsiveness of Oprm1-INs to the Oprm1-selective agonist DAMGO was dramatically reduced by SNI.

Third, SNI increased membrane excitability, synaptic activity, and gene expression in Oprm1-INs. Fourth, chemogenetic activation of spinal Oprm1-INs was sufficient to induce mechanical hypersensitivity in naïve mice. Fifth, chemogenetic inhibition of spinal Oprm1-INs mitigated behavioral signs of neuropathic pain.

Molecular heterogeneity of Oprm1-interneuronss in the spinal dorsal horn

tdTomato-labelled Oprm1-INs were mainly distributed throughout laminae I-III, consistent with previous immunohistochemical studies describing Oprm1-immunoreactivity in superficial laminae.[12,40] Co-labeling of tdTomato with TLX3 and PAX2 revealed that roughly 60% and 40% of *Oprm1*-expressing neurons are excitatory and inhibitory neurons, respectively, consistent with recent *in situ* hybridization studies.[27–29] Inhibitory Oprm1-INs have been segregated into sub-populations expressing either neuropeptide Y, dynorphin, parvalbumin or nitric oxide synthase 1.[10,27] The neurochemical phenotypes of excitatory Oprm1-INs appear to be even more numerous.[10] Of particular interest are the results of Wang *et al* who reported that ~30% of spinal *Oprm1*-expressing neurons co-express the excitatory peptide-encoding gene *Grp* (gastrin-releasing peptide),[28] as GRP-expressing interneurons are remarkably responsiveness to DAMGO application.[25] As an overall excitatory tone of DH interneurons is thought to cause allodynia in models of cutaneous inflammation or peripheral nerve injury, whereas a net activation of inhibitory circuits produces anti-allodynia or analgesia,[41] future studies are needed to further unravel the molecular identity of subpopulations of excitatory Oprm1-INs.[41]

SNI renders spinal Oprm1-interneuronss less responsive to DAMGO

Previous studies of randomly sampled lamina II neurons reported that peripheral nerve injury reduced DAMGO inhibition of postsynaptic potassium currents and primary afferent-evoked postsynaptic currents, presumably by actions at its cognate receptor.[32] Our results confirm and extend this by showing that loss of DAMGO inhibition occurs on the Oprm1-expressing population. A frequently cited mechanism of decreased MOR agonist function is the loss of MOR expression and decreased G protein coupling to MOR,[2,32,42,43] and this is supported by our finding that SNI decreased *Oprm1* mRNA expression in DH. In contrast to nerve injury, tissue or systemic inflammation does not change or increases the expression of *Oprm1* in DH.[43,44] Perhaps for this reason, opiates are more efficacious for the clinical treatment of inflammatory pain than for neuropathic pain. In summary, our results and others indicate that nerve injury reduces the functional responsiveness of Oprm1-INs to a MOR selective agonist, perhaps via downregulation of *Oprm1*, leading to loss of opioid analgesic efficacy in the setting of long-term neuropathic pain in both preclinical animal models and clinical trials of neuropathic pain.

Spared nerve injury increases the excitability of spinal Oprm1-interneuronss

In the present study, SNI elicited multiple signs of increased excitability in Oprm1^{tdT} neurons: 1) a depolarizing shift in the resting membrane potential toward AP threshold; 2) decrease in the amount of current needed to evoke an action potential (rheobase); 3) increased frequency of spontaneous EPSCs in delayed firing Oprm1-INs, consistent with reported increases of excitatory drive (e.g. increases the spontaneous release of excitatory amino acids) onto delayed firing neurons in the spinal dorsal horn after CCI and sciatic

nerve axotomy in the rat;[24,45] and 4) increased brush-induced Fos expression in Oprm1-INs, extending previous findings of nerve injury-induced Fos expression in the superficial dorsal horn.[37,46] Together, our electrophysiological recordings of membrane properties, synaptic activity, and gene expression suggest that SNI increases the excitability of superficial DH neurons and extends previous findings to a specific subtype of labeled interneuron, the Oprm1-IN. Nerve injury may increase A fiber input to sensitized Oprm1-INs, leading to mechanical allodynia.[12,46] Future studies could determine whether nerve injury-induced hyperexcitability of Oprm1-INs is a result of increased excitatory drive and/or disinhibition of GABAergic or glycinergic neurons.[45,47,48]

Dorsal horn *Oprm1*-expressing neuron contribute to neuropathic hypersensitivity

Previous studies indicate a critical role for spinal excitatory interneurons in the transmission of pain-like behavior[5–7,46] and our results point to Oprm1-INs as an important sub-population; chemogenetics-facilitated cell type-specific activation of Oprm1-INs elicited mechanical hypersensitivity in naive mice, while inhibition reduced mechanical and cold hypersensitivity associated with peripheral nerve injury. Previous studies of acute pain indicate that ablation of spinal Oprm1-INs with intrathecal administration of dermorphin-saporin reduced the antinociceptive effects of morphine.[40] By contrast, our studies of neuropathic pain avoided pitfalls associated with lesion-associated toxicity and circuit rearrangements. Interestingly, we find that inhibition of Oprm1-INs reduces pain-like behavior even though *Oprm1* expression is found in excitatory and inhibitory interneurons. Our chemogenetic manipulations suggest that excitatory Oprm1-INs functionally predominate in the DH (this is also supported by the larger relative proportion of the number of excitatory to inhibitory Oprm1-INs as shown in Figure 4F). Future studies may begin to discriminate between the function of excitatory vs inhibitory Oprm1-IN subpopulations. For example, researchers might use a dual recombinase strategy and selectively modulate excitatory or inhibitory Oprm1-INs (one example is to generate $Oprm1^{Cre:GFP}$::Vglut2^{FlpO} mice and target with Cre/Flp dependent rAAV chemogenetic vectors). A similar strategy could study inhibitory subpopulations. Such experiments would begin to reveal the functional role of excitatory vs. inhibitory Oprm1-INs. In summary, we propose that Oprm1-INs are an important subpopulation of excitatory interneurons that contribute to neuropathic pain-like behavior and are the site of action of DREADD inhibition with CNO. However, we cannot exclude the possibility that CNO disinhibited inhibitory Oprm1-INs that might normally function to dampen neuropathic pain.

In summary, using a reliable Oprm1^{Cre} transgenic mouse line, we reveal a robust neuroplasticity of Oprm1-INs in the setting of neuropathic pain-like behavior. Peripheral sciatic nerve injury reduced *Oprm1* gene expression and the responsiveness of Oprm1-INs to a selective μ agonist, consistent with the lack of clinical efficacy of opioid analgesics for the treatment of neuropathic pain. As illustrated with a conceptual summary (Figure 10), nerve injury not only potentiated light brush-induced expression of Fos in Oprm1-INs, but also increased their intrinsic excitability and spontaneous synaptic activity, indicating the development of neuronal sensitization. Chemogenetic activation of Oprm1-INs produced mechanical allodynia, while chemogenetic inhibition reduced behavioral signs of neuropathic pain. We conclude that peripheral nerve injury sensitizes a pro-nociceptive

population of Oprm1-INs that contributes to neuropathic pain-like behavior and propose that non-opioid strategies to inhibit Oprm1-INs is a promising approach to treat neuropathic pain.

Supplementary Material

Refer to Web version on PubMed Central for supplementary material.

Acknowledgments

We thank Professor Dr. Richard Palmiter, Ph.D. (University of Washington, Seattle, WA, USA) for providing the *Oprm1*^{Cre} mouse. We thank Dr. Diogo F.S. Santos, PhD (University of Pittsburgh School of Medicine, Pittsburgh, PA, USA) and Megan Lynn Schadle, MS (University of Pittsburgh School of Medicine, Pittsburgh, PA, USA) for technical support on mouse behavioral assays. We also thank Ronald Sivak, BS (Department of Anesthesiology and Perioperative Medicine, University of Pittsburgh School of Medicine, Pittsburgh, PA, USA) for genotyping the mouse lines.

Funding Statement:

This work was supported by National Institute of Health grants R01DA37621, R01NS45954, R01NS62306, The Pittsburgh Foundation, The Raymond and Elizabeth Bloch Educational and Charitable Foundation (B.K.T); and by NIH grants T32NS073548, F31NS117054, and F99NS124190 (T.S.N.)

References

1. Todd AJ: Neuronal circuitry for pain processing in the dorsal horn. Nat Rev Neurosci 2010; 11: 823–36 [PubMed: 21068766]
2. Taylor BK: Pathophysiologic mechanisms of neuropathic pain. Curr Pain Headache Rep 2001; 5: 151–61 [PubMed: 11252149]
3. Corder G, Doolen S, Donahue RR, Winter MK, Jutras BL, He Y, Hu X, Wieskopf JS, Mogil JS, Storm DR, Wang ZJ, McCarson KE, Taylor BK: Constitutive mu-opioid receptor activity leads to long-term endogenous analgesia and dependence. Science 2013; 341: 1394–9 [PubMed: 24052307]
4. Finnerup NB, Kuner R, Jensen TS: Neuropathic Pain: From Mechanisms to Treatment. Physiol Rev 2021; 101: 259–301 [PubMed: 32584191]
5. Nelson TS, Taylor BK: Targeting spinal neuropeptide Y1 receptor-expressing interneurons to alleviate chronic pain and itch. Prog Neurobiol 2021; 196: 101894
6. Peirs C, Williams SG, Zhao X, Arokiaraj CM, Ferreira DW, Noh MC, Smith KM, Halder P, Corrigan KA, Gedeon JY, Lee SJ, Gatto G, Chi D, Ross SE, Goulding M, Seal RP: Mechanical Allodynia Circuitry in the Dorsal Horn Is Defined by the Nature of the Injury. Neuron 2021; 109: 73–90 e7 [PubMed: 33181066]
7. Duan B, Cheng L, Bourane S, Britz O, Padilla C, Garcia-Campmany L, Krashes M, Knowlton W, Velasquez T, Ren X, Ross S, Lowell BB, Wang Y, Goulding M, Ma Q: Identification of spinal circuits transmitting and gating mechanical pain. Cell 2014; 159: 1417–1432 [PubMed: 25467445]
8. Mantyh PW, Rogers SD, Honore P, Allen BJ, Ghilardi JR, Li J, Daughters RS, Lappi DA, Wiley RG, Simone DA: Inhibition of hyperalgesia by ablation of lamina I spinal neurons expressing the substance P receptor. Science 1997; 278: 275–9 [PubMed: 9323204]
9. Nelson TS, Sinha GP, Santos DFS, Jukkola P, Prasoon P, Winter MK, McCarson KE, Smith BN, Taylor BK: Spinal neuropeptide Y Y1 receptor-expressing neurons are a pharmacotherapeutic target for the alleviation of neuropathic pain. Proc Natl Acad Sci U S A 2022; 119: e2204515119
10. Todd AJ: Identifying functional populations among the interneurons in laminae I-III of the spinal dorsal horn. Mol Pain 2017; 13: 1744806917693003
11. Kemp T, Spike RC, Watt C, Todd AJ: The mu-opioid receptor (MOR1) is mainly restricted to neurons that do not contain GABA or glycine in the superficial dorsal horn of the rat spinal cord. Neuroscience 1996; 75: 1231–8 [PubMed: 8938756]

12. Wang D, Tawfik VL, Corder G, Low SA, Francois A, Basbaum AI, Scherrer G: Functional Divergence of Delta and Mu Opioid Receptor Organization in CNS Pain Circuits. Neuron 2018; 98: 90–108 e5 [PubMed: 29576387]
13. Stein C: Opioid Receptors. Annu Rev Med 2016; 67: 433–51 [PubMed: 26332001]
14. Corder G, Castro DC, Bruchas MR, Scherrer G: Endogenous and Exogenous Opioids in Pain. Annu Rev Neurosci 2018; 41: 453–473 [PubMed: 29852083]
15. Cooper AH, Hedden NS, Corder G, Lamerand SR, Donahue RR, Morales-Medina JC, Selan L, Prasoon P, Taylor BK: Endogenous micro-opioid receptor activity in the lateral and capsular subdivisions of the right central nucleus of the amygdala prevents chronic postoperative pain. J Neurosci Res 2022; 100: 48–65 [PubMed: 33957003]
16. Nelson TS, Fu W, Donahue RR, Corder GF, Hokfelt T, Wiley RG, Taylor BK: Facilitation of neuropathic pain by the NPY Y1 receptor-expressing subpopulation of excitatory interneurons in the dorsal horn. Sci Rep 2019; 9: 7248 [PubMed: 31076578]
17. Chaplan SR, Bach FW, Pogrel JW, Chung JM, Yaksh TL: Quantitative assessment of tactile allodynia in the rat paw. J Neurosci Methods 1994; 53: 55–63 [PubMed: 7990513]
18. Sinha GP, Prasoon P, Smith BN, Taylor BK: Fast A-type currents shape a rapidly adapting form of delayed short latency firing of excitatory superficial dorsal horn neurons that express the neuropeptide Y Y1 receptor. J Physiol 2021; 599: 2723–2750 [PubMed: 33768539]
19. Basu P, Custodio-Patsey L, Prasoon P, Smith BN, Taylor BK: Sex Differences in Protein Kinase A Signaling of the Latent Postoperative Pain Sensitization That Is Masked by Kappa Opioid Receptors in the Spinal Cord. J Neurosci 2021; 41: 9827–9843 [PubMed: 34531285]
20. Uceyler N, Tscharke A, Sommer C: Early cytokine expression in mouse sciatic nerve after chronic constriction nerve injury depends on calpain. Brain Behav Immun 2007; 21: 553–60 [PubMed: 17204395]
21. Vandesompele J, De Preter K, Pattyn F, Poppe B, Van Roy N, De Paepe A, Speleman F: Accurate normalization of real-time quantitative RT-PCR data by geometric averaging of multiple internal control genes. Genome Biol 2002; 3: RESEARCH0034
22. Schneider SP, Eckert WA 3rd, Light AR: Opioid-activated postsynaptic, inward rectifying potassium currents in whole cell recordings in substantia gelatinosa neurons. J Neurophysiol 1998; 80: 2954–62 [PubMed: 9862898]
23. Ruscheweyh R, Sandkuhler J: Lamina-specific membrane and discharge properties of rat spinal dorsal horn neurones in vitro. J Physiol 2002; 541: 231–44 [PubMed: 12015432]
24. Balasubramanyan S, Stemkowski PL, Stebbing MJ, Smith PA: Sciatic chronic constriction injury produces cell-type-specific changes in the electrophysiological properties of rat substantia gelatinosa neurons. J Neurophysiol 2006; 96: 579–90 [PubMed: 16611846]
25. Dickie AC, Bell AM, Iwagaki N, Polgar E, Gutierrez-Mecinas M, Kelly R, Lyon H, Turnbull K, West SJ, Etlin A, Braz J, Watanabe M, Bennett DLH, Basbaum AI, Riddell JS, Todd AJ: Morphological and functional properties distinguish the substance P and gastrin-releasing peptide subsets of excitatory interneuron in the spinal cord dorsal horn. Pain 2019; 160: 442–462 [PubMed: 30247267]
26. Yasaka T, Tiong SYX, Hughes DI, Riddell JS, Todd AJ: Populations of inhibitory and excitatory interneurons in lamina II of the adult rat spinal dorsal horn revealed by a combined electrophysiological and anatomical approach. Pain 2010; 151: 475–488 [PubMed: 20817353]
27. Nguyen E, Lim G, Ding H, Hachisuka J, Ko MC, Ross SE: Morphine acts on spinal dynorphin neurons to cause itch through disinhibition. Sci Transl Med 2021; 13
28. Wang Z, Jiang C, Yao H, Chen O, Rahman S, Gu Y, Zhao J, Huh Y, Ji RR: Central opioid receptors mediate morphine-induced itch and chronic itch via disinhibition. Brain 2021; 144: 665–681 [PubMed: 33367648]
29. Zhang XY, Dou YN, Yuan L, Li Q, Zhu YJ, Wang M, Sun YG: Different neuronal populations mediate inflammatory pain analgesia by exogenous and endogenous opioids. Elife 2020; 9
30. Zhou HY, Chen SR, Chen H, Pan HL: Sustained inhibition of neurotransmitter release from nontransient receptor potential vanilloid type 1-expressing primary afferents by mu-opioid receptor activation-enkephalin in the spinal cord. J Pharmacol Exp Ther 2008; 327: 375–82 [PubMed: 18669865]

31. Fujita T, Kumamoto E: Inhibition by endomorphin-1 and endomorphin-2 of excitatory transmission in adult rat substantia gelatinosa neurons. Neuroscience 2006; 139: 1095–105 [PubMed: 16515840]
32. Kohno T, Ji RR, Ito N, Allchorne AJ, Befort K, Karchewski LA, Woolf CJ: Peripheral axonal injury results in reduced mu opioid receptor pre- and post-synaptic action in the spinal cord. Pain 2005; 117: 77–87 [PubMed: 16098668]
33. Zain M, Bonin RP: Alterations in evoked and spontaneous activity of dorsal horn wide dynamic range neurons in pathological pain: a systematic review and analysis. Pain 2019; 160: 2199–2209 [PubMed: 31149976]
34. Latremoliere A, Woolf CJ: Central sensitization: a generator of pain hypersensitivity by central neural plasticity. J Pain 2009; 10: 895–926 [PubMed: 19712899]
35. Bullitt E: Expression of c-fos-like protein as a marker for neuronal activity following noxious stimulation in the rat. J Comp Neurol 1990; 296: 517–30 [PubMed: 2113539]
36. Ma QP, Woolf CJ: Basal and touch-evoked fos-like immunoreactivity during experimental inflammation in the rat. Pain 1996; 67: 307–16 [PubMed: 8951924]
37. Intondi AB, Dahlgren MN, Eilers MA, Taylor BK: Intrathecal neuropeptide Y reduces behavioral and molecular markers of inflammatory or neuropathic pain. Pain 2008; 137: 352–365 [PubMed: 17976913]
38. Solway B, Bose SC, Corder G, Donahue RR, Taylor BK: Tonic inhibition of chronic pain by neuropeptide Y. Proc Natl Acad Sci U S A 2011; 108: 7224–9 [PubMed: 21482764]
39. Porreca F, Burgess SE, Gardell LR, Vanderah TW, Malan TP Jr., Ossipov MH, Lappi DA, Lai J: Inhibition of neuropathic pain by selective ablation of brainstem medullary cells expressing the mu-opioid receptor. J Neurosci 2001; 21: 5281–8 [PubMed: 11438603]
40. Kline RHt, Wiley RG: Spinal mu-opioid receptor-expressing dorsal horn neurons: role in nociception and morphine antinociception. J Neurosci 2008; 28: 904–13 [PubMed: 18216198]
41. Peirs C, Dallel R, Todd AJ: Recent advances in our understanding of the organization of dorsal horn neuron populations and their contribution to cutaneous mechanical allodynia. J Neural Transm (Vienna) 2020; 127: 505–525 [PubMed: 32239353]
42. Martinez-Navarro M, Maldonado R, Banos JE: Why mu-opioid agonists have less analgesic efficacy in neuropathic pain? Eur J Pain 2019; 23: 435–454 [PubMed: 30318675]
43. Obara I, Parkitna JR, Korostynski M, Makuch W, Kaminska D, Przewlocka B, Przewlocki R: Local peripheral opioid effects and expression of opioid genes in the spinal cord and dorsal root ganglia in neuropathic and inflammatory pain. Pain 2009; 141: 283–291 [PubMed: 19147290]
44. Ballet S, Conrath M, Fischer J, Kaneko T, Hamon M, Cesselin F: Expression and G-protein coupling of mu-opioid receptors in the spinal cord and dorsal root ganglia of polyarthritic rats. Neuropeptides 2003; 37: 211–9 [PubMed: 12906839]
45. Chen Y, Balasubramanyan S, Lai AY, Todd KG, Smith PA: Effects of sciatic nerve axotomy on excitatory synaptic transmission in rat substantia gelatinosa. J Neurophysiol 2009; 102: 3203–15 [PubMed: 19793881]
46. Peirs C, Williams SP, Zhao X, Walsh CE, Gedeon JY, Cagle NE, Goldring AC, Hioki H, Liu Z, Marell PS, Seal RP: Dorsal Horn Circuits for Persistent Mechanical Pain. Neuron 2015; 87: 797–812 [PubMed: 26291162]
47. Lu VB, Biggs JE, Stebbing MJ, Balasubramanyan S, Todd KG, Lai AY, Colmers WF, Dawbarn D, Ballanyi K, Smith PA: Brain-derived neurotrophic factor drives the changes in excitatory synaptic transmission in the rat superficial dorsal horn that follow sciatic nerve injury. J Physiol 2009; 587: 1013–32 [PubMed: 19124536]
48. Moore KA, Kohno T, Karchewski LA, Scholz J, Baba H, Woolf CJ: Partial peripheral nerve injury promotes a selective loss of GABAergic inhibition in the superficial dorsal horn of the spinal cord. J Neurosci 2002; 22: 6724–31 [PubMed: 12151551]

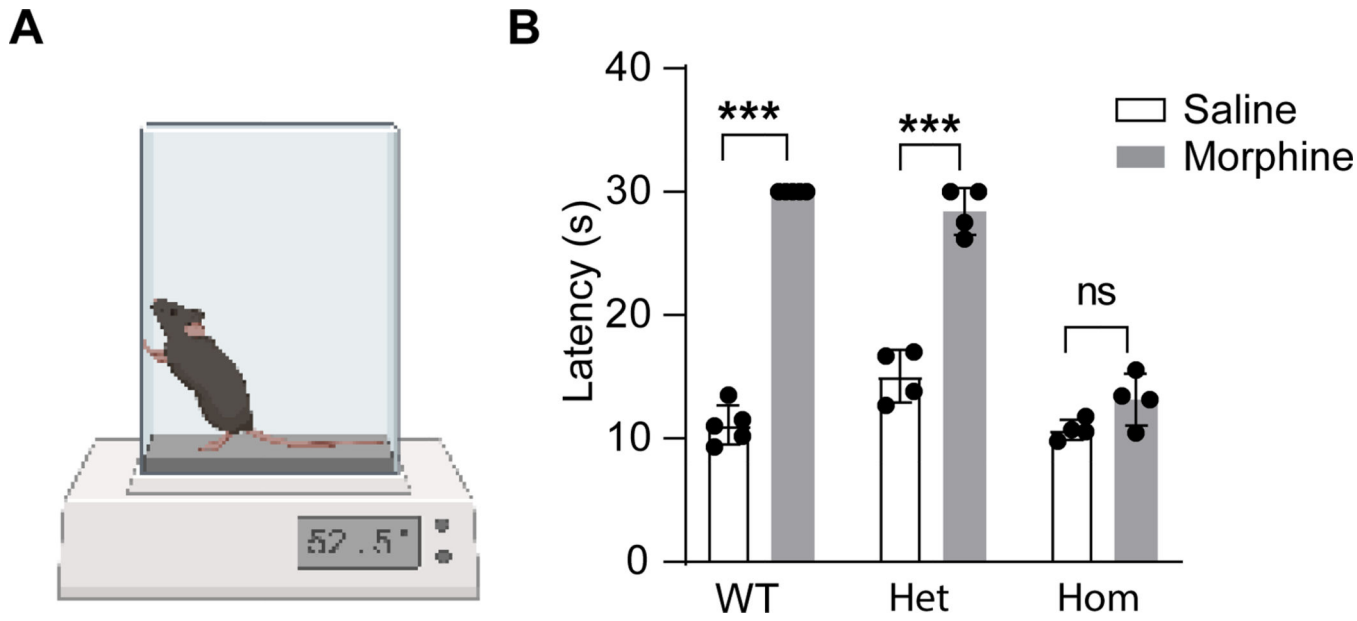

Figure 1. Morphine-induced analgesia remains largely intact in heterozygous Oprm1^{Cre} mice.
(A) Hot plate test of morphine-induced analgesia. **(B)** Paw withdrawal latency to heat when tested 30 minutes after saline or morphine (IP, 5 mg/kg) in wild-type (WT, n=5), Oprm1$^{Cre/+}$ (Het, n=4) and Oprm1$^{Cre/Cre}$ (Hom, n=4) mice. Two-way repeated measure ANOVA, $F(2, 20)=94.61$; Turkey's post hoc test: Saline (WT) vs Morphine (WT), $p < 0.0001$; Saline (Het) vs Morphine (Het), $p < 0.0001$; Saline (Hom) vs Morphine (Hom), $p = 0.28$; Data presented as mean ± SD. ***p<0.001.

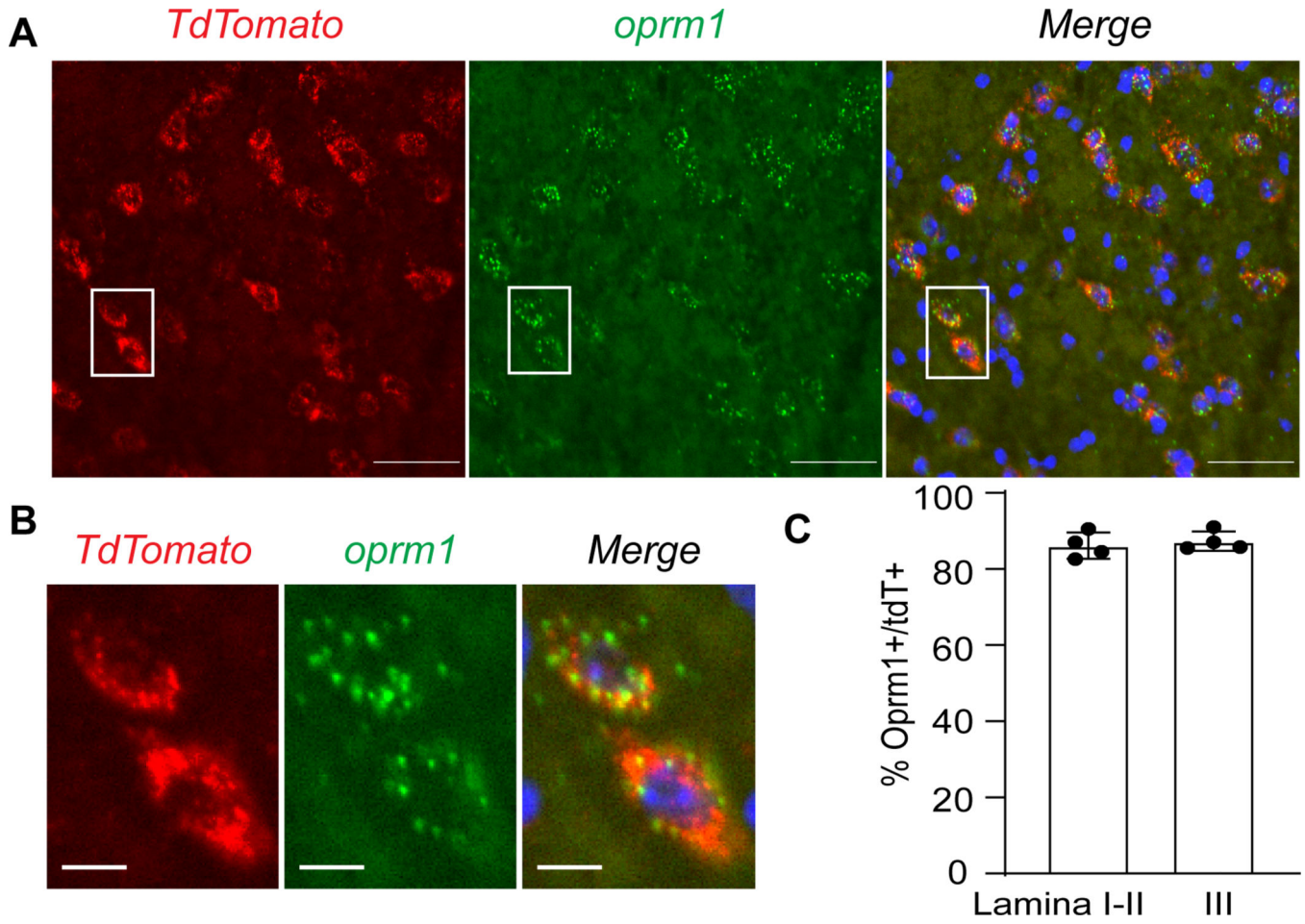

Figure 2. Oprm1^{tdT} mice recapitulate endogenous Oprm1 expression in dorsal horn.
(A) In situ hybridization of *tdTomato* mRNA (red) and *Oprm1* mRNA (green) in superficial dorsal horn of Oprm1^{tdT} mice. Scale bar = 50μm. See Fig 4D for lower power image of tdTomato expression in dorsal horn. **(B)** Magnification of insets from A. Scale bar = 10μm. **(C)** Co-expression of *Oprm1* and *tdTomato* mRNA in lamina I-II and lamina III. Data presented as mean ± SD.

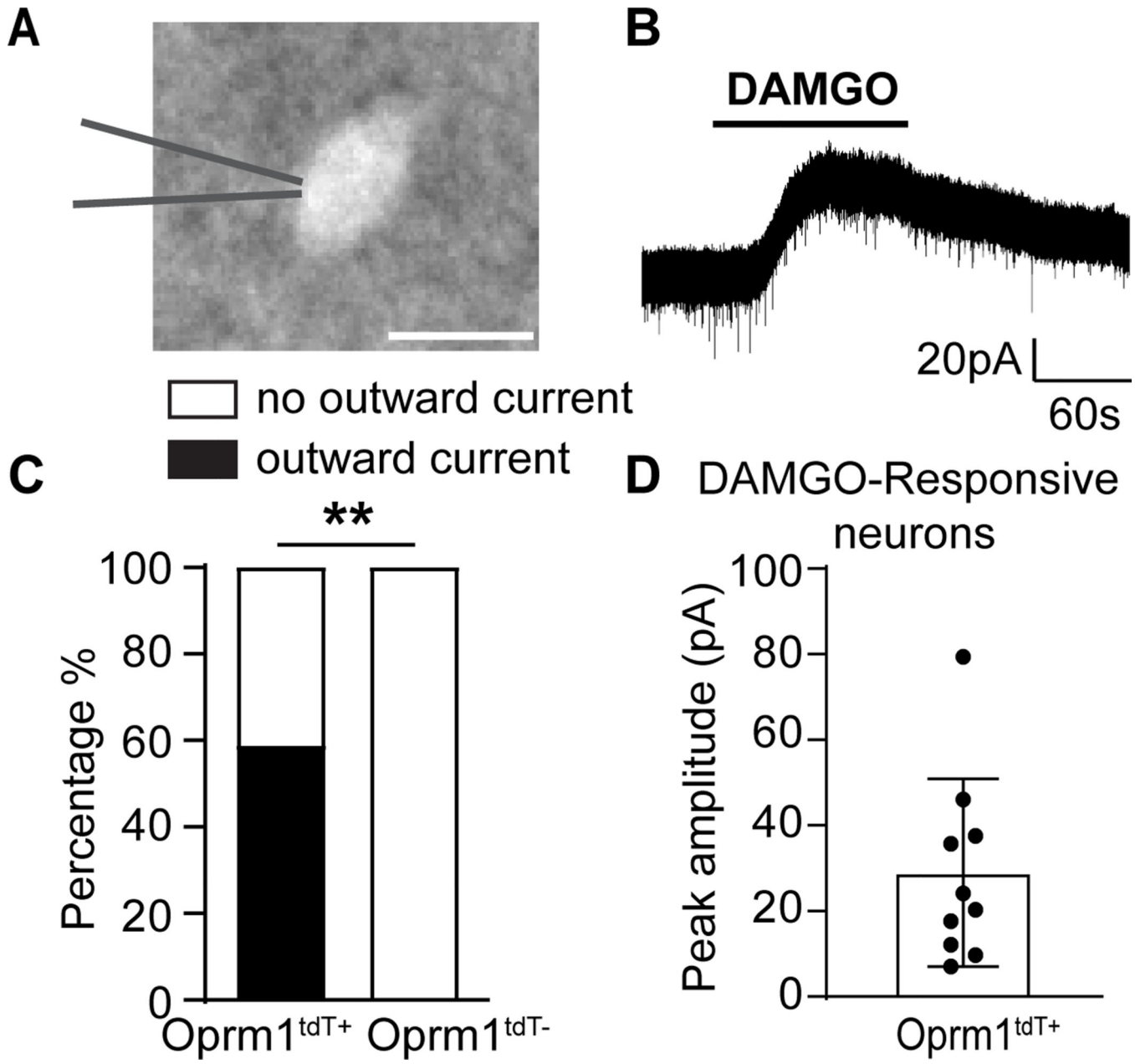

Figure 3. DAMGO induces an outward current in tdTomato-labelled Oprm1-INs.

(A) An Oprm1^{tdT+} neuron in lamina II. Scale bar: 10μm. **(B)** Representative trace and **(C)** Proportion of Oprm1^{tdT+} neurons that exhibited outward currents to DAMGO (1μM, 2 min, n=17 from 7 mice). DAMGO did not evoke responses in Oprm1^{tdT-} neurons (n=9 from 3 mice). Oprm1^{tdT+} vs Oprm1^{tdT-}; Fisher's exact test, p = 0.0039. **(D)** Mean amplitude of DAMGO-induced outward currents in Oprm1^{tdT+} neurons. Data are presented as mean ± SD. ** p<0.01.

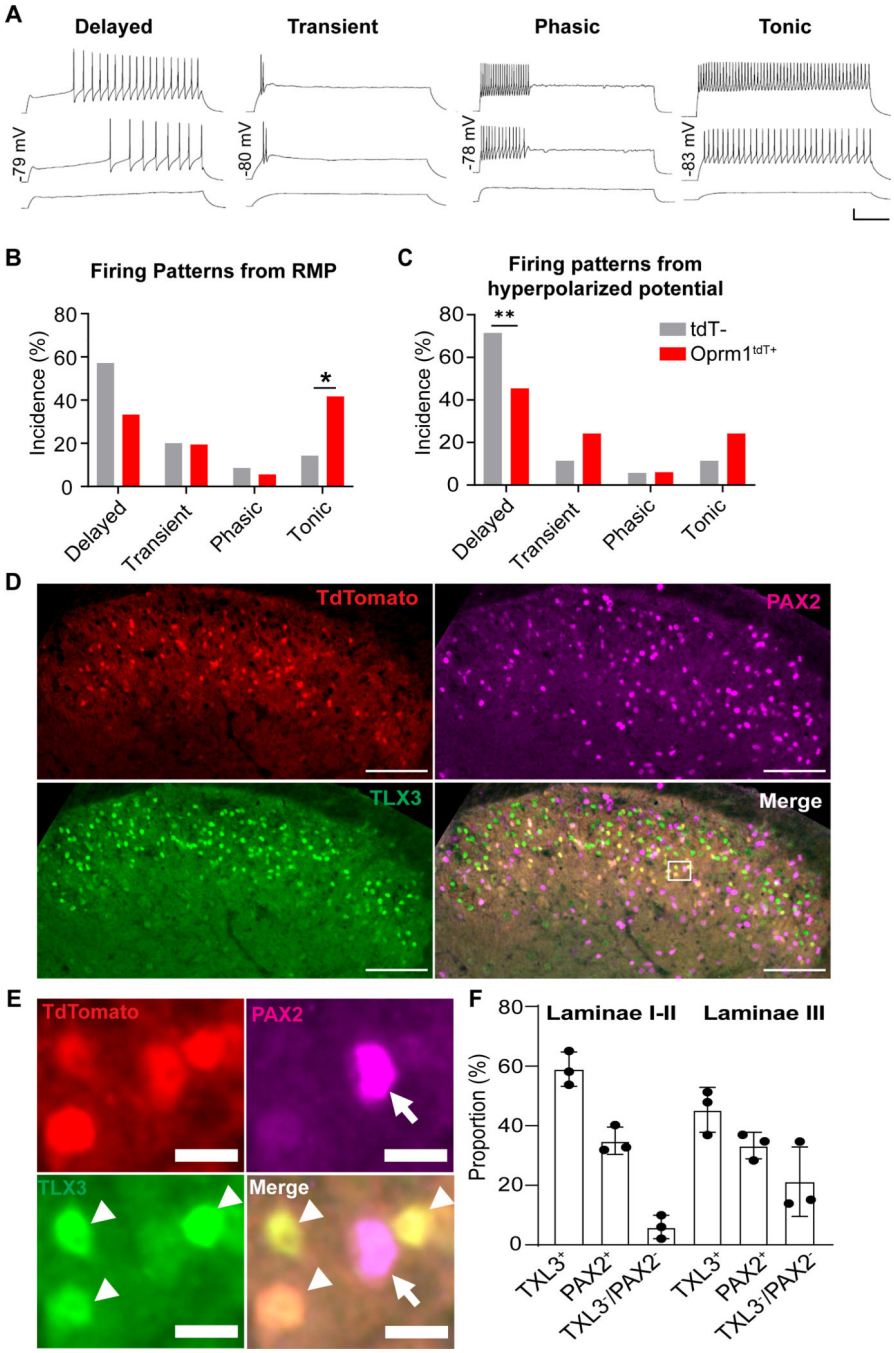

Figure 4. Heterogeneity of Oprm1^{tdT} neurons in dorsal horn.

(A) Action potential firing patterns of Oprm1^{tdT+} neurons: delayed, transient, phasic and tonic firing. Scale bars: horizontal=200ms; vertical=20mV. **(B, C)** Incidence of firing patterns elicited in tdTomato positive (Oprm1^{tdT+}) and tdTomato negative (tdT-) neurons from **(B)** resting (~−60mV, n=36 from 9 Oprm1^{tdT+} mice; n=35 from 6 tdT- mice) or **(C)** hyperpolarized (~−−80mV, Oprm1^{tdT+}: n=33 from 9 mice; tdT-: n=35 from 6 mice) membrane potentials; Oprm1^{tdT+} vs tdT-; Fisher's exact test, Tonic (in B): p = 0.0166; Delayed (in C): p = 0.0014. **(D)** Oprm1tdT+ neurons (red) co-express TLX3 (green) and

PAX2 (magenta) in the dorsal horn. Scale bar, 100 μm. **(E)** high magnification images of the white boxed areas in D. Arrows indicate double-labeled profiles of Oprm1^{tdT+} with PAX2, and arrowheads indicate double-labeled profiles of Oprm1^{tdT+} with TLX3. Scale bar, 10 μm. **(F)** Percentage of TLX3+ and PAX2+ neurons in Oprm1^{tdT+} neurons. n=10 sections from three mice. Data are presented as mean ± SD. *p<0.05, **p<0.01.

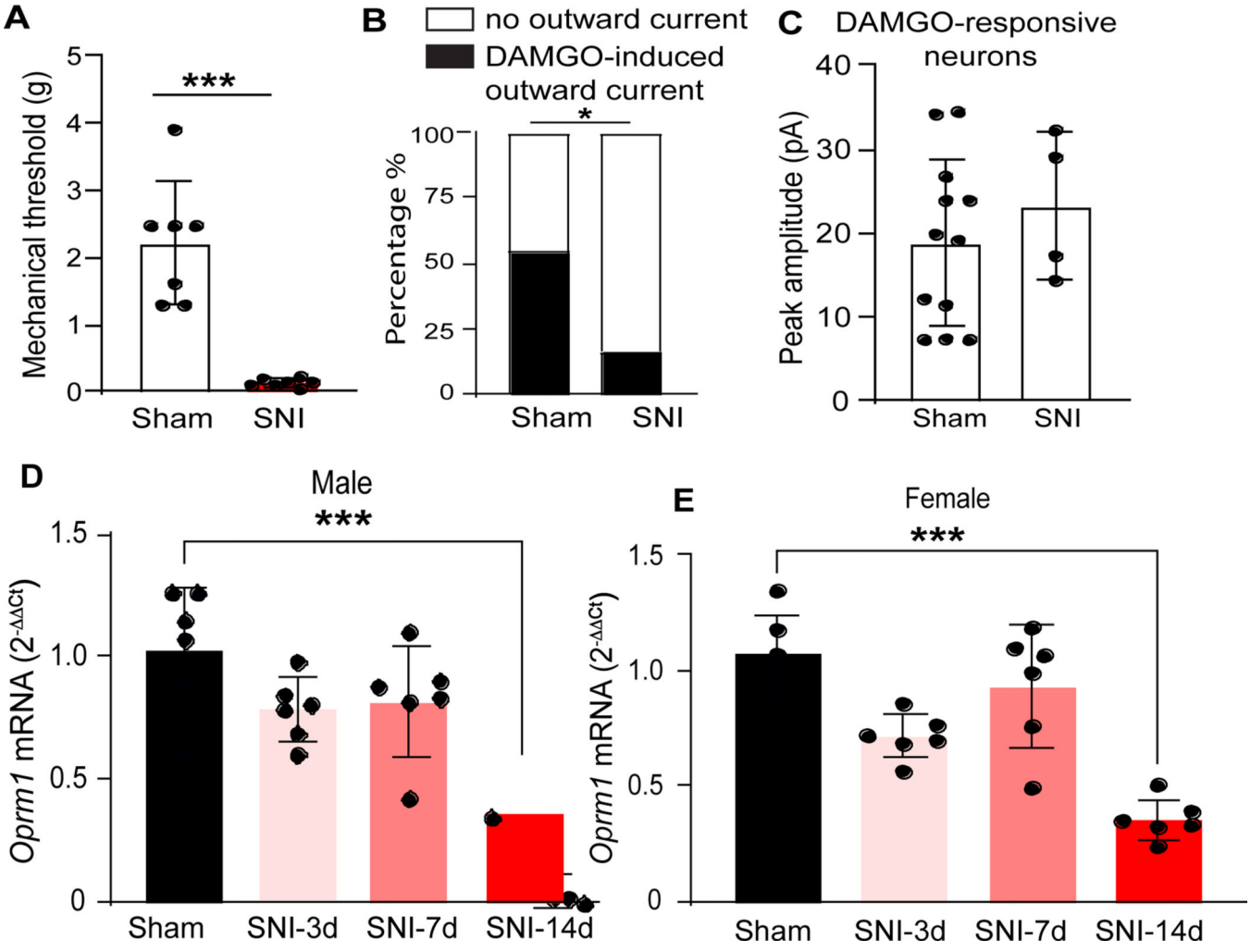

Figure 5. Spared nerve injury reduces functional responsiveness of Oprm1-interneurons to DAMGO.

(A) Mechanical thresholds in Oprm1^{tdT} mice 14 days after sham (n=7) or SNI (n=7) surgery. Sham vs SNI, unpaired t-test, p<0.0001. **(B)** Proportion of Oprm1^{tdT} neurons exhibiting DAMGO-induced outwards currents in sham (n=22 neurons from 7 mice) and SNI (n=24 neurons from 7 mice). sham vs SNI: Fisher's exact test, p=0.0124. **(C)** DAMGO-induced outward currents in sham and SNI groups. **(D)** *Oprm1* expression in male sham mice or 3, 7, or 14 days after SNI. One-way analysis of variance, F(3,20)=13.8, p<0.0001; Sham vs SNI-14d: Turkey's post hoc test, p<0.0001. (E) *Oprm1* expression in female sham mice or 3, 7, or 14 days after SNI. F(3,20)=20.3, p<0.0001; Sham vs SNI-14d: Turkey's post hoc test, p<0.0001. Data are mean ± SD. *p<0.05, ***p<0.001. SNI, spared nerve injury.

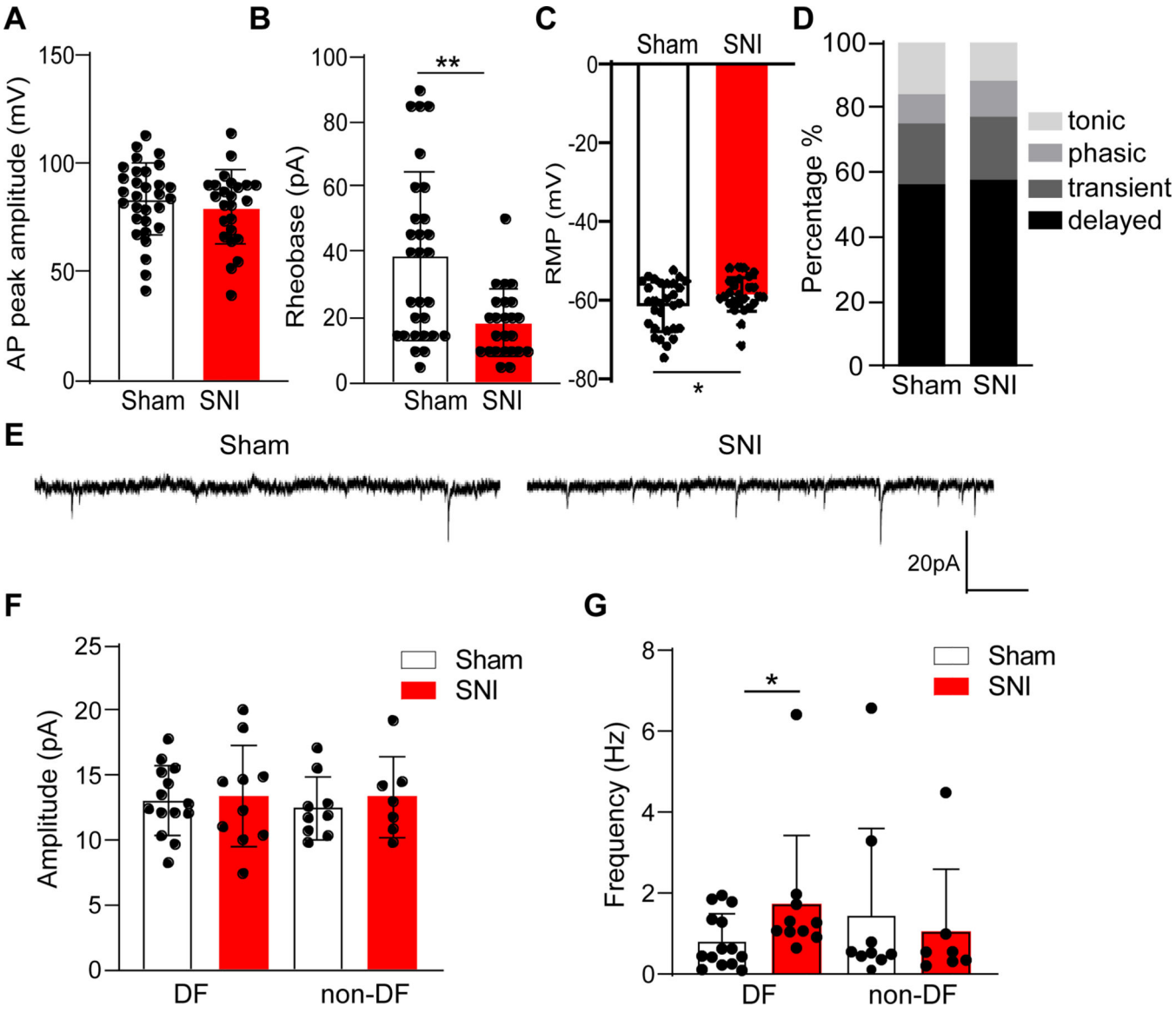

Figure 6. Spared nerve injury increases membrane excitability and synaptic activity of Oprm1^{tdT+} neurons.

(A) SNI did not change the amplitude of action potentials (Sham: n=30 Oprm1^{tdT+} neurons from 7 mice; SNI: n=24 neurons from 7 mice; p=0.45, unpaired t-test). **(B)** SNI reduced rheobase (Sham: n=29 from 7 mice; SNI: n=24 Oprm1^{tdT+} neurons from 7 mice; p=0.0016, Mann Whitney test). **(C)** SNI depolarized the resting membrane potential (Sham: n=30 Oprm1^{tdT+} from 7 mice; SNI: n=26 neurons from 7 mice; p=0.049, unpaired t-test). **(D)** SNI did not change action potential discharge. Sham: n=32 Oprm1^{tdT+} neurons from 7 mice; SNI: n=26 neurons from 7 mice; p=0.25, Chi-square test. **(E)** Representative traces of sEPSCs from delayed firing (DF) Oprm1^{tdT+} neurons in lamina II. Mean amplitude (**F**) and frequency (**G**) of sEPSCs exhibited by DF and non-delayed firing (non-DF) neurons. Sham: n=14 neurons from 7 mice; SNI: n=10 neurons from 7 mice. p=0.0466, Mann Whitney test. Data are mean ± SEM. *p<0.05, **p<0.01. SNI, spared nerve injury. sEPSC, spontaneous excitatory postsynaptic currents

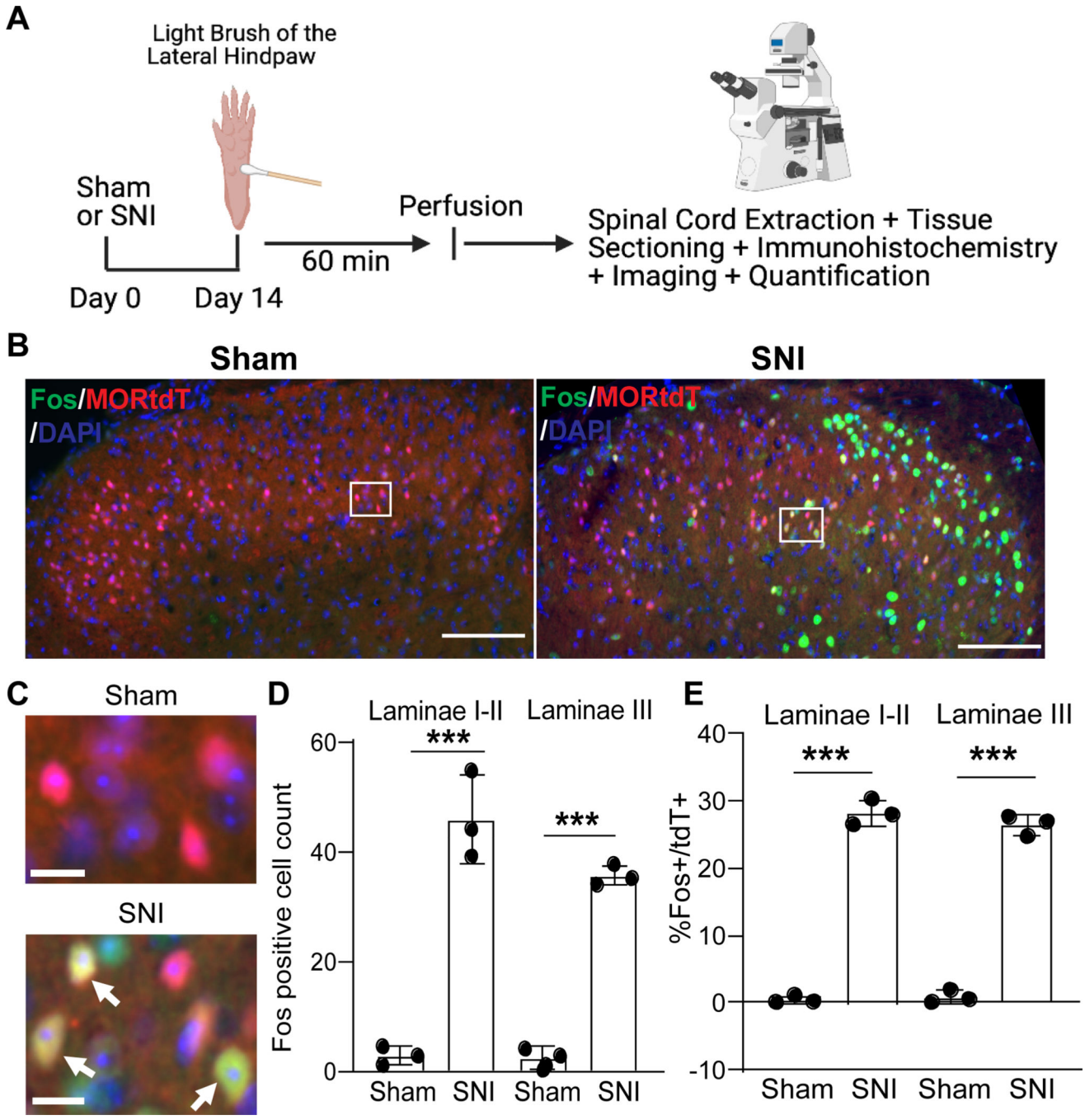

Figure 7. Spared nerve injury increases touch-evoked Fos expression in Oprm1^{tdT+} neurons.

(A) Timeline. (**B)** Representative images of Fos (green) and tdTomato (red) expression in the lumbar dorsal horn, ipsilateral to plantar application of light brush, 14 days after sham or SNI surgery. **(C)** High magnification images of the white boxed areas in B. Arrows indicate double-labeled cells. **(D)** Quantification of brush-evoked Fos at the ipsilateral laminae I-II and III dorsal horn neurons after sham and SNI. Sham compared to SNI: F (3,6)=90.78; Laminae I-II ($p<0.0001$): Lamina III ($p=0.002$); Turkey's post-hoc test in two-way analysis of variance. **(E)** Percentage of Oprm1tdT+ neurons that are Fos-immunoreactive at the

ipisilateral laminae I-II and III dorsal horn neurons after sham and SNI. Sham compared to SNI: Laminae I-I ($p<0.0001$); Lamina III ($p<0.0001$); Turkey's post-hoc test in two-way ANOVA. Ten spinal cord sections from three mice were analyzed for each group. Scale bar,100 μm in (B) and 10 μm in (C). ***$p < 0.001$. Data are presented as mean ± SD. SNI, spared nerve injury.

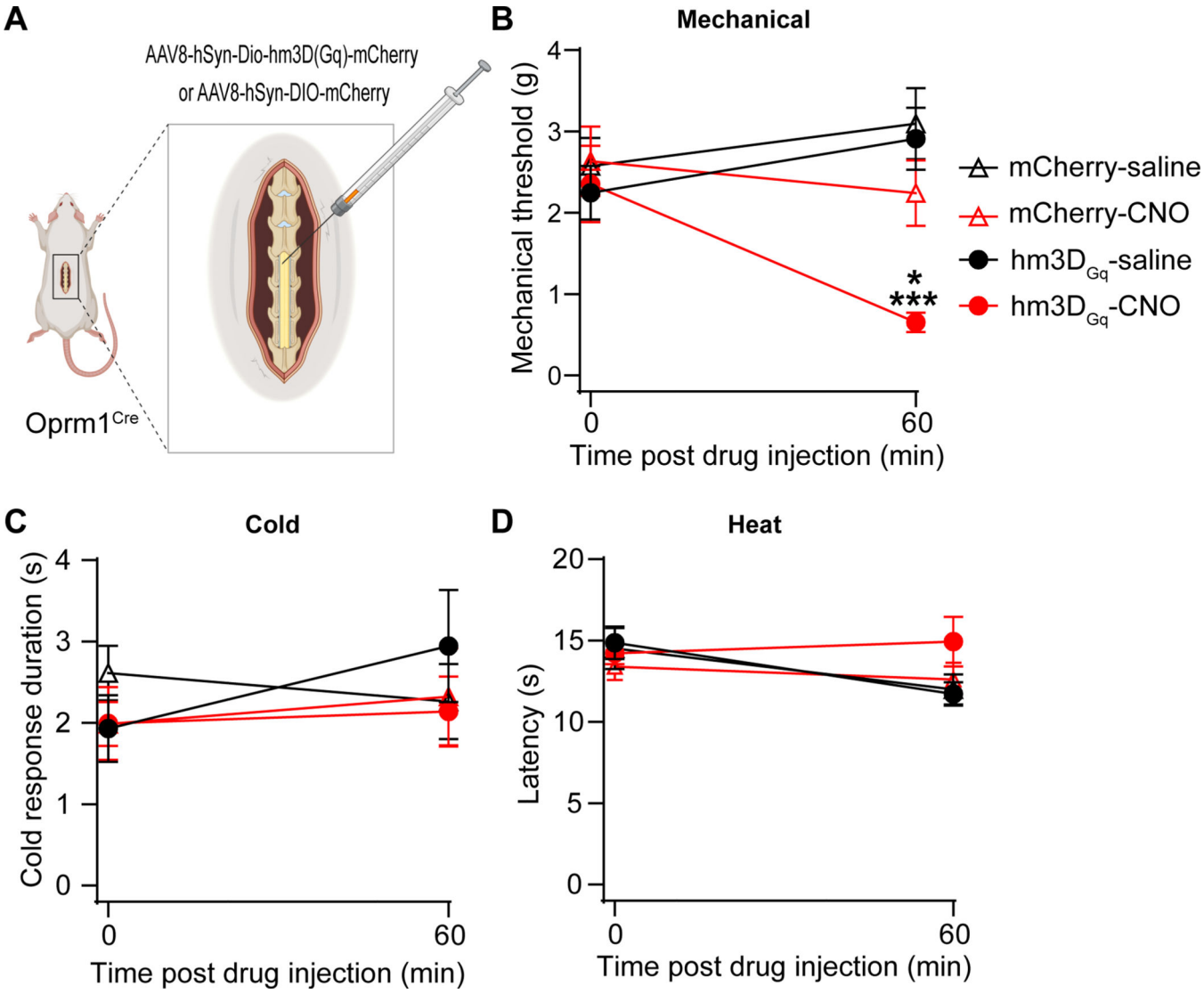

Figure 8. Chemogenetic activation of spinal Oprm1-interneuronss induces mechanical hypersensitivity.

(A) Intraspinal injection of AAV8-hSyn-DIO-hM3D(Gq)-mCherry (hM3D$_{Gq}$) or control AAV8-hSyn-DIO-mCherry (mCherry) virus into male Oprm1^{Cre} mice. **(B)** Mechanical thresholds before and 60min after injection of saline or CNO (IP, 3mg/kg) in hM3D$_{Gq}$ mice (n=8) or their mCherry controls (n=8). hM3D$_{Gq}$-saline vs hM3D$_{Gq}$-CNO, p=0.0005; hM3D$_{Gq}$-CNO vs mCherry-CNO, p=0.0175; hM3D$_{Gq}$-CNO (0min) vs hM3D$_{Gq}$-CNO (60min) p=0.0006; **(C and D)** CNO did not change cold response duration (C) or heat sensitivity (D). Holm-Sidak post hoc test after two-way RM ANOVA, *p<0.05 hM3D$_{Gq}$-CNO vs mCherry-CNO, ***p<0.001 hM3D$_{Gq}$-saline vs hM3D$_{Gq}$-CNO. CNO, clozapine-N-oxide.

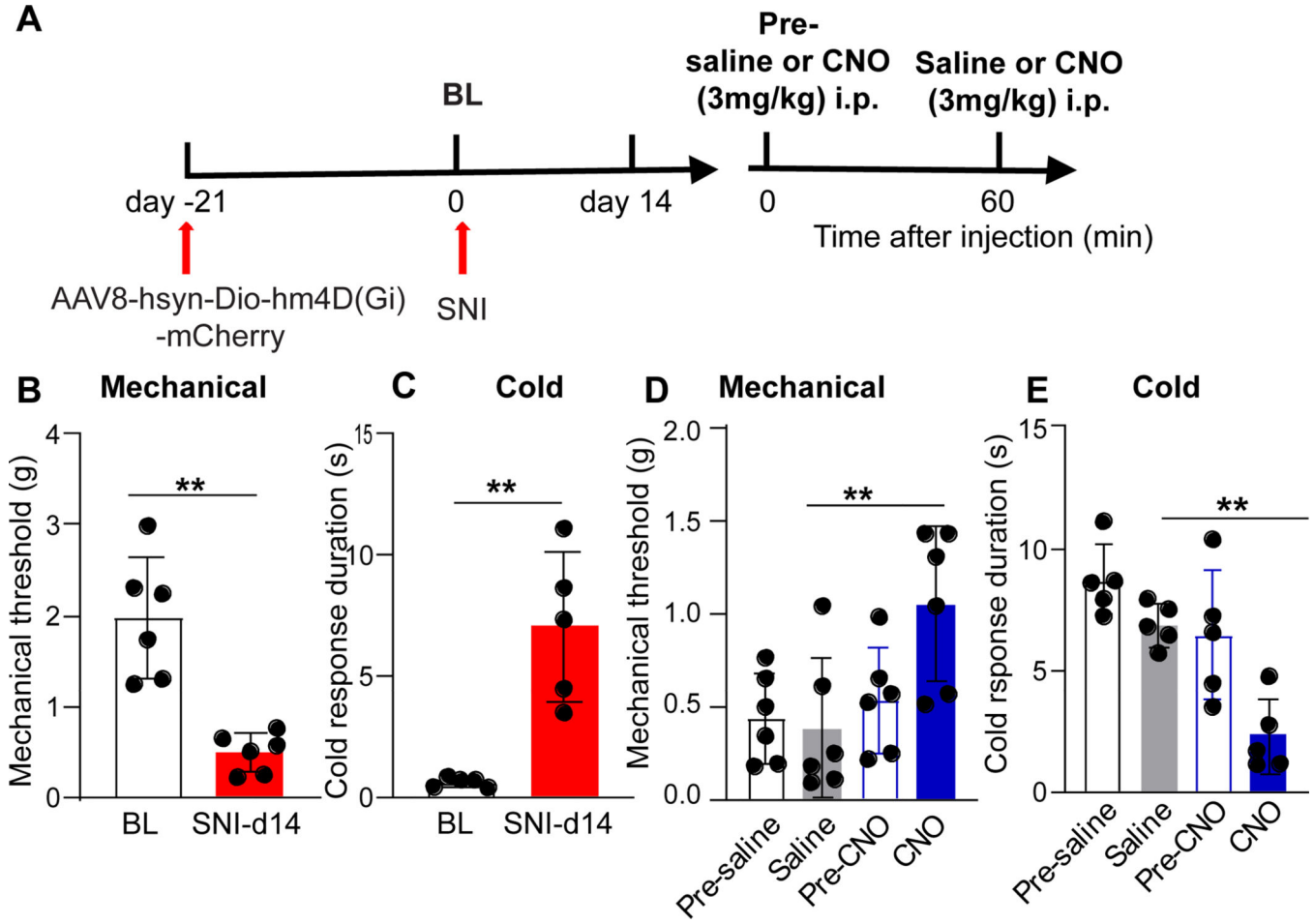

Figure 9. Chemogenetic inhibition of Oprm1-interneuronss reduces neuropathic pain.

(A) Experimental timeline of surgery and CNO injection after intraspinal injection of AAV8-hSyn-DIO-hM4D(Gi)-mCherry ($hM4D_{Gi}$) virus into male $Oprm1^{Cre}$ mice. Mechanical thresholds **(B)** and cold response duration **(C)** before and 14 days after SNI. **p<0.01, Student's t-test. Mechanical thresholds **(D)** and cold response duration **(E)** before and after injection of saline or CNO, 14 days after SNI. Mechanical: Pre-CNO vs CNO, p=0.0074; saline vs CNO, p=0.0052; Pre-CNO vs CNO, p=0.0025; Cold: saline vs CNO, p=0.0017; Holm-Sidak post hoc test after two-way RM ANOVA, **p<0.01. n=5–6 per group. Data are presented as mean ± SD. CNO, clozapine-N-oxide.

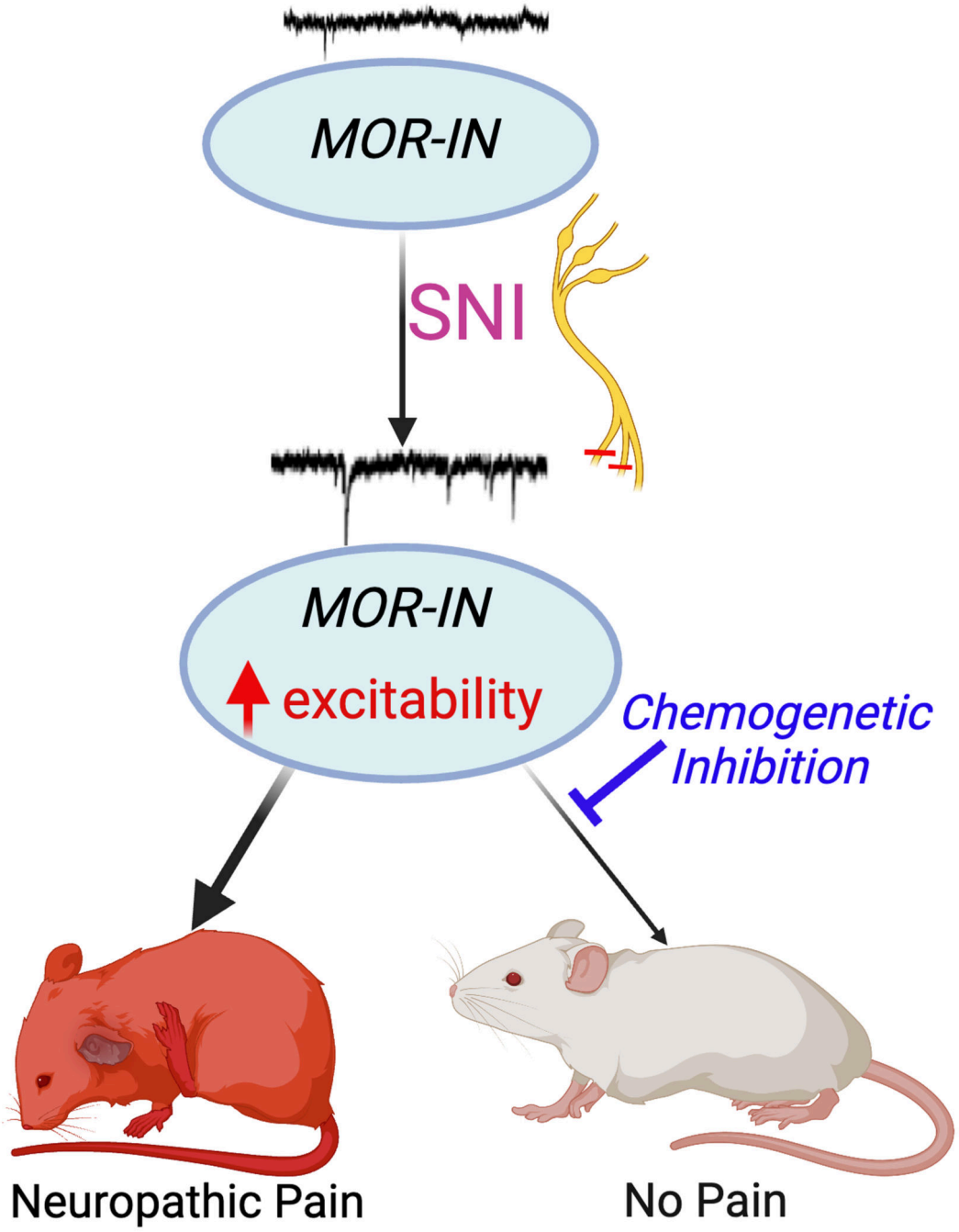

Figure 10.

Conceptual summary of conclusions from the current date. The SNI of neuropathic pain increases the excitability of mu opioid receptor-expressing interneurons (Oprm1-INs). This is associated with neuropathic pain-like behaviors (red mouse). Chemogenetic inhibition of Oprm1-INs reduces behaviors (white mouse), suggesting that Oprm1-INs contribute to neuropathic pain. Created with BioRender.com. SNI, spared nerve injury; IN, interneuron

Table 1.

Passive membrane properties of Oprm1tdT positive and tdT negative neurons in the spinal dosal horn.

	Oprm1tdT+ (n=49)	**tdT- (n=35)**
Membrane capacitance (pF)	23.52±1.30	26.16±1.27
Input resistance (MΩ)	1054±81.2	1096±99.38
RMP (mV)	−60.29±1.02	−60.56±0.96

Oprm1tdT: n=49 from 10 mice, tdT-: n=35 from 6 mice. p>0.05, Student's t-test, Data are mean ± SEM.

Table 2.

Effects of SNI on passive membrane properties of Oprm1tdTneurons in the spinal dosal horn

	Sham	SNI
Membrane capacitance (pF)	21.73±1.54 (n=25)	20.90±1.45 (n=26)
Input resistance (MΩ)	1234±109 (n=33)	1262±116.7 (n=25)

Data were collected from 7 sham and 7 SNI Oprm1tdT mice, $p>0.05$, Student's t-test, Data are mean ± SEM.